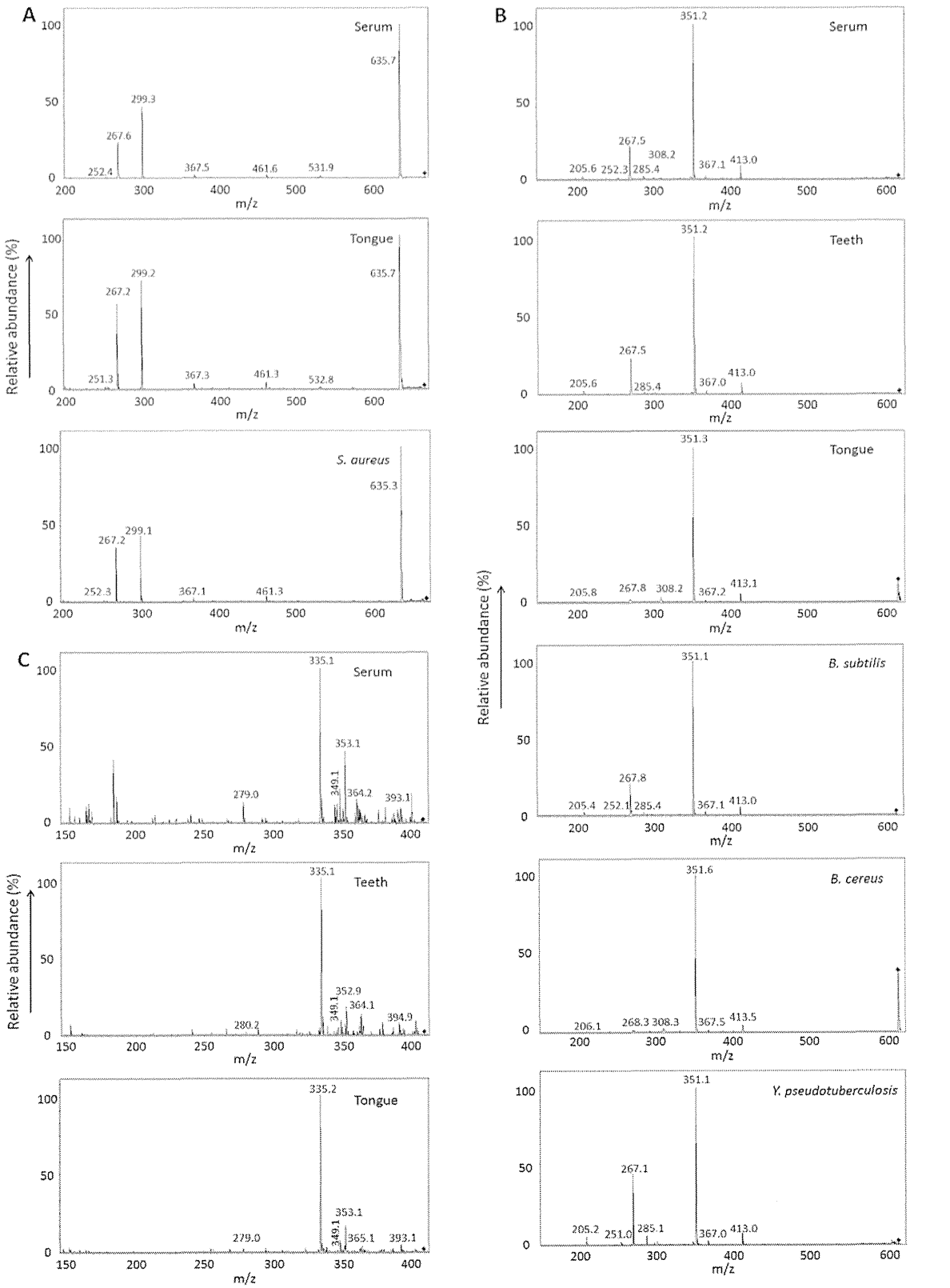
A
Serum
635.7
299.3
267.6
252.4
367.5
461.6
531.9
Tongue
635.7
299.2
267.2
251.3
367.3
461.3
532.8
S. aureus
635.3
299.1
267.2
252.3
367.1
461.3
B
Serum
351.2
267.5
308.2
205.6
252.3
285.4
367.1
413.0
Teeth
351.2
267.5
205.6
285.4
367.0
413.0
Tongue
351.3
205.8
267.8
308.2
367.2
413.1
B. subtilis
351.1
267.8
205.4
252.1
285.4
367.1
413.0
B. cereus
351.6
206.1
268.3
308.3
367.5
413.5
Y. pseudotuberculosis
351.1
267.1
205.2
251.0
285.1
367.0
413.0
C
Serum
335.1
353.1
349.1
279.0
364.2
393.1
Teeth
335.1
352.9
349.1
364.1
280.2
394.9
Tongue
335.2
353.1
349.1
279.0
365.1
393.1
Relative abundance (%)
m/z

**Figure 4. KD *in vivo* biofilms contain MAMPs common to serum KD-specific molecules (3rd study period).** Three serum KD-specific molecules (m/z 667.4, 619.4 and 409.3) at the 3rd study showed the same m/z with MS/MS fragmentation patterns similar to MAMPs from *in vivo* biofilm extracts (Table S4 in File S1) and *in vitro* bacterial biofilm extracts. A: The molecule at m/z 667.4 was common in KD serum, tongue biofilm extracts and *in vitro* biofilm extracts from *S. aureus*. B: The molecule at m/z 619.4 was common in KD serum, teeth and tongue biofilm extracts, and *in vitro* biofilm extracts from *B. subtilis*, *B. cereus* and *Y. pseudotuberculosis*. C: The molecule at m/z 409.3 was common in KD serum, and teeth and tongue biofilm extracts.
doi:10.1371/journal.pone.0113054.g004

molecules were conducted on KD and DC samples. Three KD-specific IgG sepharose-binding molecules were detected in KD sera of the 1st study period. One (m/z 1414.3) of the 5 serum KD-specific MAMPs (Figure 5A) and 2 other serum KD-specific MAMPs (m/z 745.6, 733.2) were detected in the IgG sepharose-binding fractions. The latter two were minor KD-specific MAMPs because they were detected in KD serum samples only after IgG sepharose purification. The MS/MS fragmentation patterns of the 3 molecules were similar to those of biofilm lipid extracts from *B.cereus*, while that of a molecule at m/z 733.2 also showed some similarity to that from *Y. pseudotuberculosis* (Figure S3 in File S1). To determine the IgG binding region of KD-specific MAMPs, polyclonal IgG, monoclonal IgG, $F(ab')_2$, and Fc affinity columns were employed. Serum KD-specific MAMPs bound to IgG mainly via Fab non antigen-binding regions (Figure 5B).

### Studies on the *in vitro* biofilm MAMPs from various microbes

We investigated the stimulatory effects of extracts from culture supernatants or *in vitro* biofilms from various microbes on HCAECs. The biofilm extracts from *B. cereus* (9 out of 9 strains), *B. subtilis* (2 out of 5), *Y. pseudotuberculosis* (4 out of 4), *Pseudomonas (P.) aeruginosa* and *S. aureus* robustly induced the production of IL-8 and/or IL-6 by HCAECs, especially when microbes were cultured in the presence of sterilized butter (Figure 6). Biofilm extracts from *B. cereus*, *B. subtilis*, *Y. pseudotuberculosis*, *P. aeruginosa* and *S. aureus* were further fractionated by HPLC. In all of these 5 bacteria, HCAEC-stimulatory activity was observed in the same fractions (Figure 7). LC-MS analysis revealed that there were no common MAMPs in the fractions with high HCAEC-stimulatory activity among the biofilm extracts from *Y. pseudotuberculosis*, *B. cereus*, *B. subtilis*, *S. aureus* and *P. aeruginosa*.

## Discussion

The present study showed that serum KD-specific molecules had distinct m/z and MS/MS fragmentation patterns in each temporal clustering of outbreaks. These findings are consistent with the fact that cases in each cluster share similar clinical features [21].

At the 1st study period, we detected 5 KD-specific molecules in patients' sera that were common to MAMPs from *in vitro* biofilms (4 from *B. cereus*, and 1 from *Y. pseudotuberculosis/S. aureus*). At the 2nd and 3rd study periods, we detected 4 and 3 serum KD-specific molecules in patients' sera, respectively, common to MAMPs from *in vivo* biofilms (1 from *B. cereus*, 1 from *B. subtilis/B. cereus/Y. pseudotuberculosis*, and 1 from *S. aureus*) in the respective KD patients. Although *Y. pseudotuberculosis* is sometimes involved in KD development [15,16], the detection rate of *Y. pseudotuberculosis*-type MAMPs was low in our study. Rather, *B. cereus*-type MAMPs were most frequently associated with KD, and indeed *B. cereus* itself was isolated from our patients. In addition, microbes producing *B. subtilis*-type and *S. aureus*-type MAMPs were also associated with KD.

*B. cereus*, *B. subtilis*, *Y. pseudotuberculosis*, *S. aureus*, and *P. aeruginosa* produced endothelial cell-activating MAMPs only in the biofilm-forming conditions, mostly in higher amounts in the presence of butter (Figure 6). Four of the 5 bacteria were isolated from our KD patients, and *P. aeruginosa* was associated with KD development [22] and isolated from the small intestine of KD patients [23].

The biofilm formation may be found in living tissues including teeth, tongue, respiratory tract, middle ears, and gastrointestinal tract [24]. In KD, specific MAMPs were detected in sera as well as in the *in vivo* biofilm extracts from various sites by LC-MS analysis. Several molecules common to both KD patients' *in vivo* biofilms and sera were not present in the *in vitro* biofilm extracts of a single microbe, probably because they were products from polymicrobial biofilms *in vivo* [25]. The transition from the planktonic state to the sessile state in the biofilm induces a radical change in the gene and protein expression in bacteria. The biofilm matrix, composed of polysaccharides, proteins, nucleic acids and lipids, is newly produced and secreted to form the immediate extracellular environment [26]. Indeed, bacterial biofilm products were reported to induce a distinct inflammatory response in human cells compared to their planktonic counterparts [27]. In our study, not culture supernatants but biofilm extracts induced cytokine production in human endothelial cells (Figure 6).

*Bacillus* species including *B. cereus* and *B. subtilis* are volatile spore-forming rods widely distributed in soil and air, and sometimes induce infections and intoxications [28,29]. The necessity of the biofilm and a certain environmental condition might explain why the presence of *Bacillus* species in control individuals does not induce KD by itself, and why other types of *Bacillus* species infections such as bacteremia and meningitis are not associated with KD development. In addition, just like KD [2], there is no person to person transmission in *Bacillus* species-associated human diseases such as food poisoning [28] and anthrax [30].

At least some serum KD-specific MAMPs bound to IgG mainly via Fab non antigen-binding regions, just like other microbial glycolipids that showed a high binding affinity to human IgG via Fab constant regions [19,20]. Therefore, it is likely that high-dose IVIGs work, at least in part, as a scavenger of such MAMPs from the blood stream, a previously unrecognized mechanism in KD [31,32].

The main limitations of our study were that the structural analysis of these KD-specific MAMPs was hampered by the instability of the lipophilic molecules after purification, and that

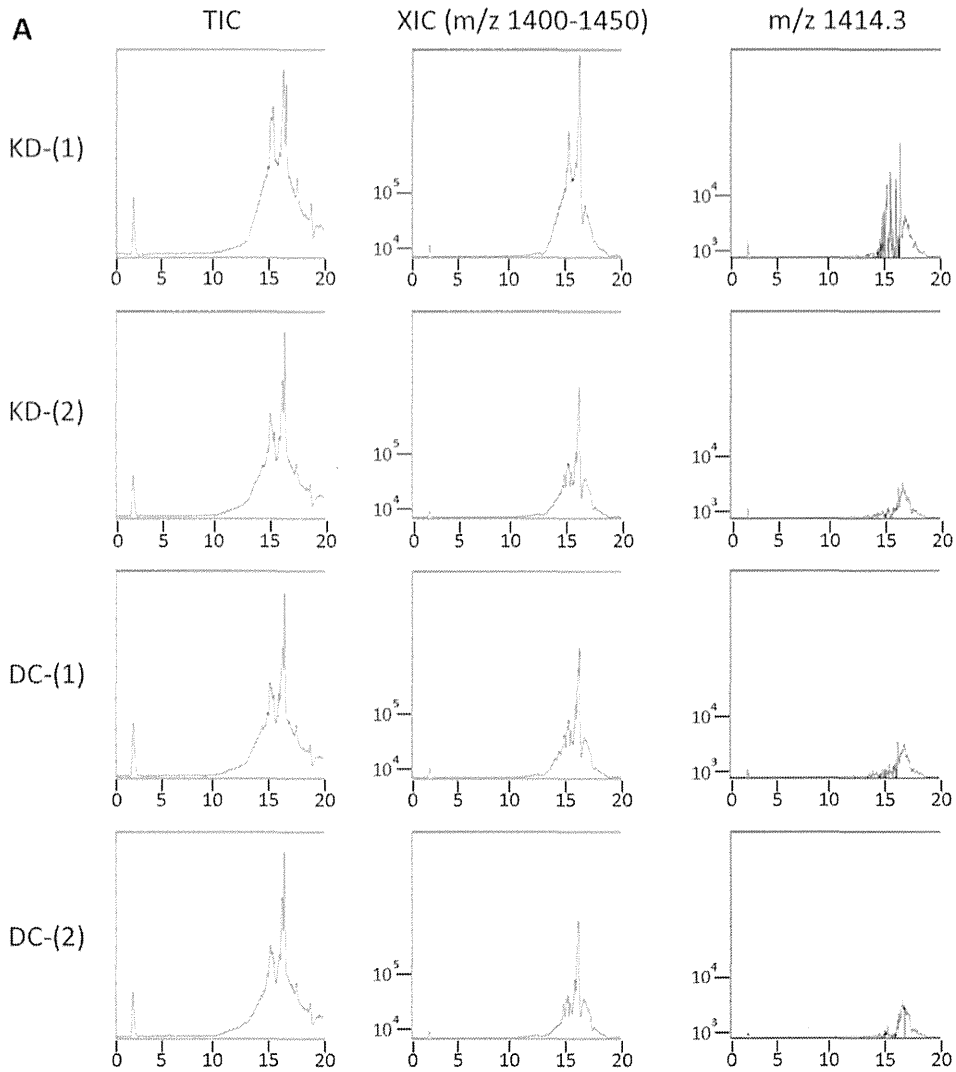


B

| Affinity column | Binding of a KD specific molecule |
|---|---|
| Human polyclonal IgG column | + |
| Mouse monoclonal IgG column | + |
| Rabbit monoclonal IgG column | + |
| Human IgG F(ab')$_2$ column | + |
| Human Fc-column | ± |
| Control column | − |

**Figure 5. LC-MS chromatograms of IgG sepharose-binding molecules.** A. Representative LC-MS chromatograms of a IgG sepharose-binding molecule (m/z 1414.3) are shown in a KD patient and a DC control. TIC: Total ion current chromatograms, XIC: Extracted-ion chromatograms at m/z 1400–1500, and extracted-ion chromatograms at m/z 1414.3. (1) Human polyclonal IgG-conjugated sepharose 6 Fast (2) Inactivated CNBr Sepharose 4B control column. B. Binding of a KD-specific molecule to various affinity columns: Columns used are described in ONLINE METHODS. +: The binding quantities of a KD-specific molecule analyzed by LC-MS were equal or larger than those to human polyclonal IgG column, ±: smaller than 20% of those to human polyclonal IgG column, -: no binding. We performed the experiments 3 times.
doi:10.1371/journal.pone.0113054.g005

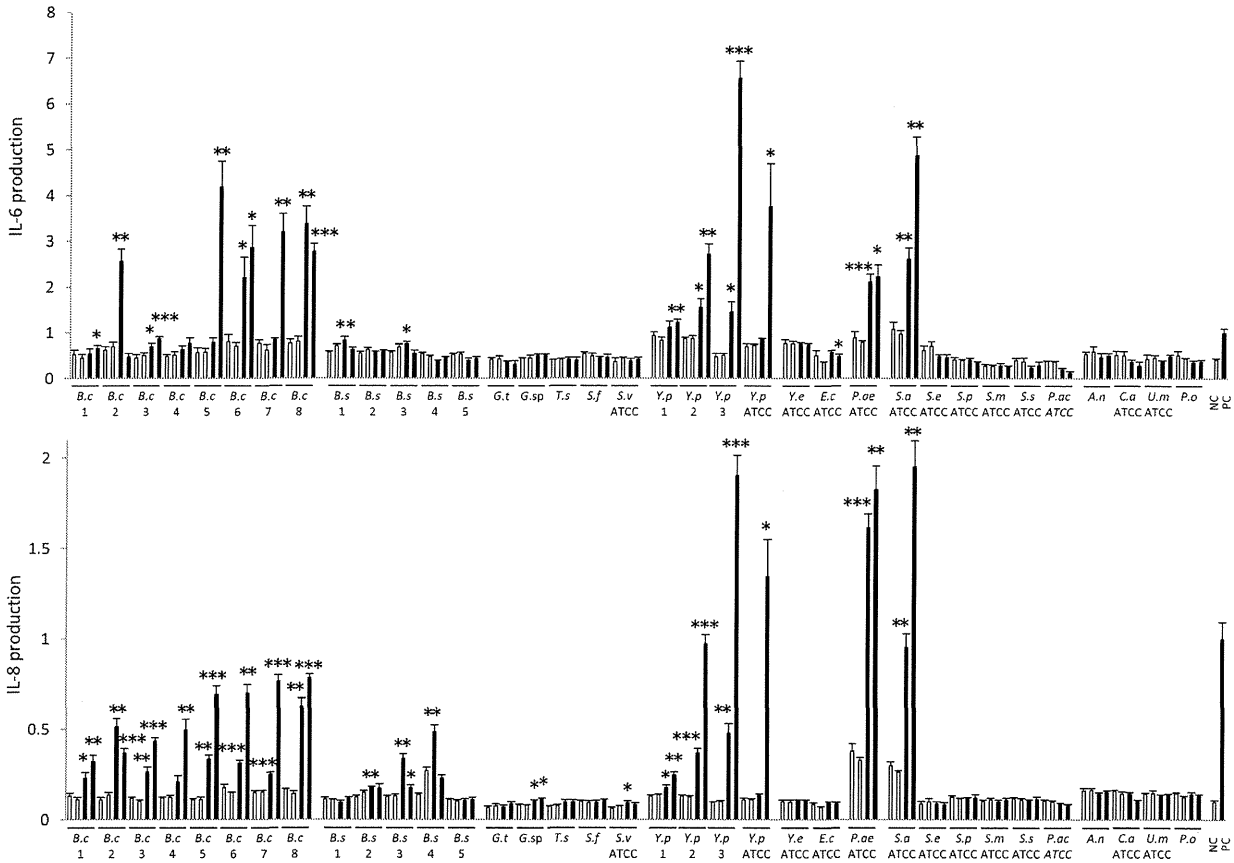


**Figure 6. Activation of HCAECs by biofilm lipid extracts from various microbes.** The production of IL-6 and IL-8 by HCAECs was measured after 24-h culture in the presence or absence of a microbial stimulant. Each microbe was cultured in the presence or absence of biofilm-forming glass slides with or without butter. As a microbial stimulant, an extract from a culture supernatant (□) or a biofilm (■) of a microbe cultured in the presence (right column) or absence (left column) of butter was used. Medium alone, ethyl acetate alone or ethyl acetate extract from glass slides cultured in the absence of a microbe was used as a negative control (NC). FK 565 (10 μg/mL) was used as a positive control (PC). *B.c: Bacillus cereus, B.s: Bacillus subtilis, G.t: Gordonia terrae, T.s: Terribacillus saccharophilus, S.f: Streptomyces flavogriseus, S.v: Streptomyces violaceus, Y.p: Yersinia pseudotuberculosis, Y.e: Yersinia enterocolitica, E.c: Escherichia coli, P.ae: Pseudomonas aeruginosa, S.a: Staphylococcus aureus, S.e: Staphylococcus epidermidis, S.p: Streptococcus pyogenes, S.m: Streptococcus mitis, S.s: Streptococcus sanguinis, P.ac: Propionibacterium acnes, A.n: Aspergillus niger, C.a: Candida albicans, U.m: Ustilago maydis, P.o: Penicillium oxalicum.* Numbers under bacteria indicate those of KD patients. Data are expressed as the fold change induction of IL-8 or IL-6 compared to the PC levels. We performed the experiments 3 times. Biofilms were compared with supernatant control considering presence or absence of butter. *$P<0.01$, **$P<0.001$ and ***$P<0.0001$ (Welch's *t*-test).
doi:10.1371/journal.pone.0113054.g006

fractionated crude biofilm extracts were too toxic to replicate the KD phenotype in mice.

We have shown that serum KD-specific molecules were diverse but mostly derived from biofilms and possessed molecular structures common to MAMPs. The present study suggests a possibility that KD-specific MAMPs induce vascular inflammation, leading to the development of KD. Further study is on the way as a nation-wide project to investigate a pathogenic link between KD development and biofilm-derived MAMPs.

## Conclusion

Extensive analysis by LC-MS/MS revealed that serum KD-specific molecules possessed molecular structures common to MAMPs from *Bacillus cereus, Bacillus subtilis, Yersinia pseudotuberculosis and Staphylococcus aureus*. These molecules were mostly derived from biofilms formed *in vivo* (teeth, tongue, nasal cavity, or stool). This report might offer novel insight into the diagnosis and management of KD as well as its pathogenesis.

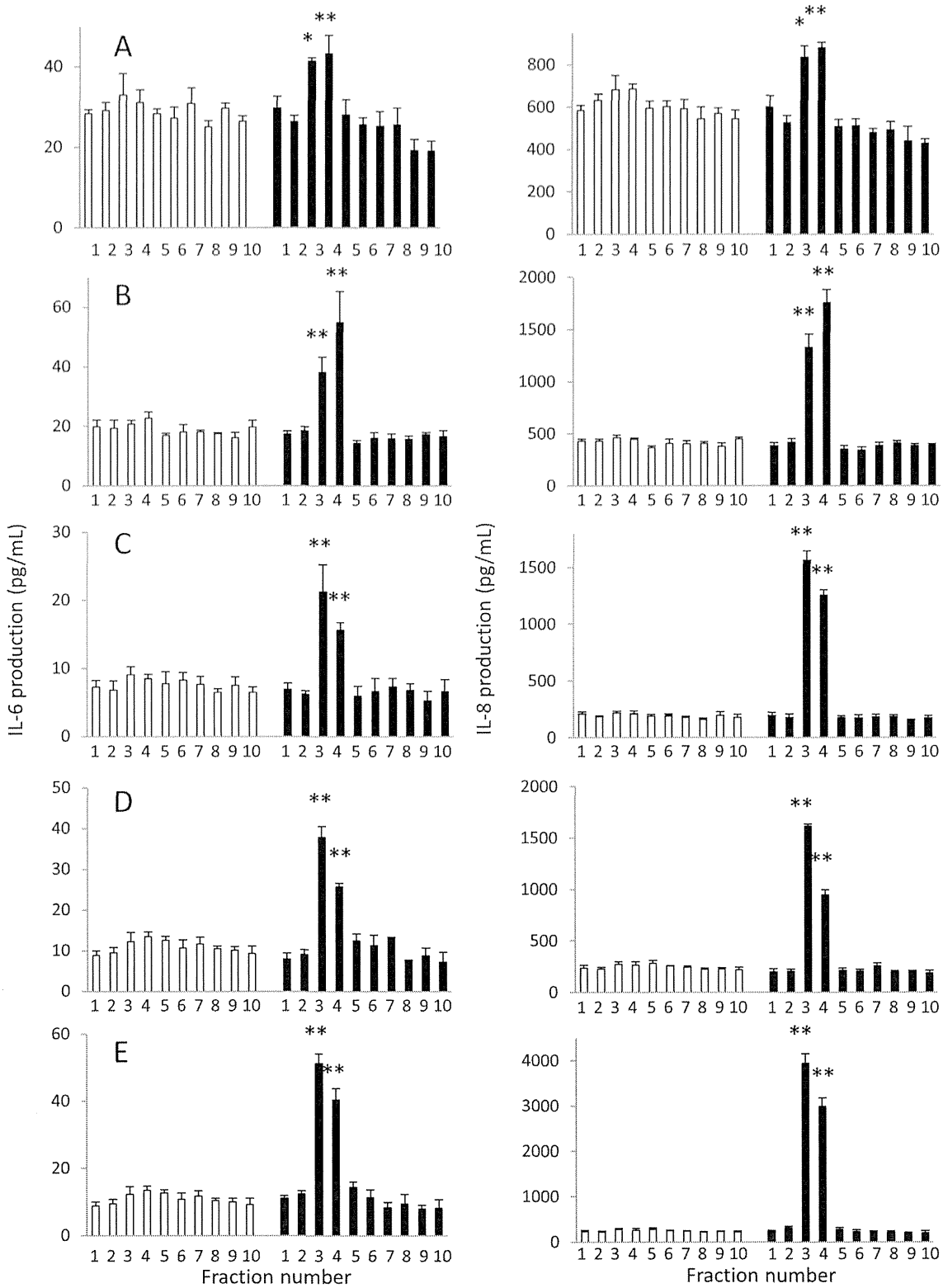


**Figure 7. Fractionation of HCAEC-activating biofilm lipid extracts by HPLC.** Each biofilm lipid extract from *Y. pseudotuberculosis* (A), *B. cereus* (B), *B. subtilis* (C), *S. aureus* (D) or *P. aeruginosa* (E) was separated into 10 fractions by HPLC and assayed for the stimulatory activity of HCAECs (■). Fractions 3 and 4 from each biofilm lipid extract induced high cytokine production by HCAECs. Ethyl acetate lipid extracts from glass slides in the

absence of microbes served as negative controls (□). Results are representative of 3 independent experiments. The stimulatory effects of fractionated biofilm samples were compared with those of corresponding controls. *$P<0.05$, **$P<0.01$ (Welch's *t*-test).
doi:10.1371/journal.pone.0113054.g007

## Supporting Information

**File S1 Supporting information.** Text S1, Supporting Materials and Methods. Figure S1, LC-MS chromatograms and the detection rates and time course of 5 KD-specific molecules. Figure S2, Effects of biofilm formation, shaking time and various oils on the production of a KD-specific MAMP by LC-MS analysis. Figure S3, LC-MS and MS/MS analyses of 3 KD-specific molecules with IgG sepharose-binding activity. Table S1, Detection rates of spore-forming and pathogenic microbes in the oral cavity and upper respiratory tract of KD patients. Table S2, Presence of MAMPs in various microbes similar to serum KD-specific molecules. Table S3, Common MAMPs between the *in vivo* biofilms and sera in respective KD patients at the 2nd study. Table S4, Common MAMPs between the *in vivo* biofilms and sera, and microbes detected in respective KD patients at the 3rd study. Table S5, Sequences of oligonucleotide primers used for the amplification microbial genes.
(PDF)

## Acknowledgments

We thank patients with Kawasaki disease and their families, pediatricians and nurses who participated in this study. The authors are also thankful to T. Abe, Fukuoka Children's Hospital for technical assistance, and S. Tokunaga, Medical Information Center, Kyushu University Hospital for statistical analyses.

## Author Contributions

Conceived and designed the experiments: TH. Performed the experiments: TK YN KM SK HN TT. Analyzed the data: TK YN KM HN TM TH. Contributed reagents/materials/analysis tools: TK YN KY YM KO KW. Wrote the paper: TK YN TH. Scientific input and contributed to discussion: MS YS HT.

## References

1. Uehara R, Belay ED (2012) Epidemiology of Kawasaki disease in Asia, Europe, and the United States. J Epidemiol 22: 79–85.
2. Newburger JW, Takahashi M, Gerber MA, Gewits MH, Tani LY, et al. (2004) Diagnosis, treatment, and long-term management of Kawasaki disease: a statement for health professionals from the Committee on Rheumatic Fever, Endocarditis and Kawasaki Disease, Council on Cardiovascular Disease in the Young, American Heart Association. Circulation 110: 2747–2771.
3. Burns JC (2007) The riddle of Kawasaki disease. N Engl J Med 356: 659–661.
4. Rodó X, Ballester J, Cayan D, Melish ME, Nakamura Y, et al. (2011) Association of Kawasaki disease with tropospheric wind patterns. Sci Rep 1: 152.
5. Foell D, Ichida F, Vogl T, Yu X, Chen R, et al. (2003) S100A12 (EN-RAGE) in monitoring Kawasaki disease. Lancet 361: 1270–1272.
6. Popper SJ, Shimizu C, Shike H, Kanegaye JT, Newburger JW, et al. (2007) Gene-expression patterns reveal underlying biological processes in Kawasaki disease. Genome Biol 8: R261.
7. Ikeda K, Yamaguchi K, Tanaka T, Mizuno Y, Hijikata A, et al. (2010) Unique activation status of peripheral blood mononuclear cells at acute phase of Kawasaki disease. Clin Exp Immunol 160: 246–255.
8. Nishio H, Kanno S, Onoyama S, Ikeda K, Tanaka T, et al. (2011) Nod1 ligands induce site-specific vascular inflammation. Arterioscler Thromb Vasc Biol 31: 1093–1099.
9. Ayusawa M, Sonobe T, Uemura S, Ogawa S, Nakamura Y, et al. (2005) Revision of diagnostic guidelines for Kawasaki disease (the 5th revised edition). Pediatr Int 47: 232–234.
10. Folch J, Lees M, Sloane Stanley GH (1957) A simple method for the isolation and purification of total lipides from animal tissues. J Biol Chem 226: 497–509.
11. Carrillo PG, Mardaraz C, Pitta-Alvarez SI, Giulietti AM (1996) Isolation and selection of biosurfactant-producing bacteria. World J Microbiol Biotechnol 12: 82–86.
12. Onghena M, Geens T, Goosens E, Wijnants M, Pico Y, et al. (2011) Analytical characterization of mannosylerythritol lipid biosurfactants produced by biosynthesis based on feedstock sources from the agrofood industry. Anal Bioanal Chem 400: 1263–1275.
13. Cyberlipid Center (2011) Lipid extraction. Available: http://www.cyberlipid.org/extract/extr0001.htm. Accessed 2011 December 10.
14. Leung DY, Cotran RS, Kurt-Jones E, Burns JC, Newburger JW, et al. (1989) Endothelial cell activation and high interleukin-1 secretion in the pathogenesis of acute Kawasaki disease. Lancet 2: 1298–1302.
15. Vincent P, Salo E, Skurnik M, Fukushima H, Simonet M (2007) Similarities of Kawasaki disease and Yersinia pseudotuberculosis infection epidemiology. Pediatr Infect Dis J 26: 629–631.
16. Tahara M, Baba K, Waki K, Arakaki Y (2006) Analysis of Kawasaki disease showing elevated antibody titres of Yersinia pseudotuberculosis. Acta Paediatr 95: 1661–1664.
17. Christie WW (2011) Rhamnolipids, sophorolipids and other glycolipid biosurfactants: Structures, occurrence and biology. The AOCS lipid library. Available: http://lipidlibrary.aocs.org/Lipids/rhamno/index.htm. Accessed 2011 November 2.
18. Abdel-Mawgoud AM, Lépine F, Déziel E (2010) Rhamnolipids. diversity of structures, microbial origins and roles. Appl Microbiol Biotechnol 86: 1323–1336.
19. Im JH, Nakane T, Yanagishita H, Ikegami T, Kitamoto D (2001) Mannosylerythritol lipid, a yeast extracellular glycolipid, shows high binding affinity towards human immunoglobulin G. BMC Biotechnolss 1: 5.
20. Ito S, Imura T, Fukuoka T, Morita T, Sakai H, et al. (2007) Kinetic studies on the interactions between glycolipid biosurfactant assembled monolayers and various classes of immunoglobulins using surface plasmon resonance. Colloids Surf B Biointerfaces 58: 165–171.
21. Yeung RS (2005) Pathogenesis and treatment of Kawasaki's disease. Curr Opin Rheumatol 17: 617–623.
22. Keren G, Cohen BE, Barzilay Z, Hiss J, Wolman M (1979) Kawasaki disease and infantile polyarteritis nodosa: is Psedomonas infection responsible? Report of a case. Isr J Med Sci 15: 592–600.
23. Yamashiro Y, Nagata S, Ohtsu Y, Oguchi S, Shimizu T (1996) Microbiologic studies on the small intestine in Kawasaki disease. Pediatr Res 39: 622–624.
24. Moran AP, Annuk H (2003) Recent Advances in Understanding Biofilms of Mucosae. Rev Environ Sci Biotechnol 2: 121–140.
25. Peters BM, Jabra-Rizk MA, O'May GA, Costerton JW, Shirtliff ME (2012) Polymicrobial interactions: impact on pathogenesis and human disease. Clin Microbiol Rev 25: 193–213.
26. Flemming HC, Wingender J (2010) The biofilm matrix. Nat Rev Microbiol 8: 623–633.
27. Secor PR, James GA, Fleckman P, Olerud JE, Mclnnerney K, et al. (2011) Staphylococcus aureus Biofilm and Planktonic cultures differentially impact gene expression, mapk phosphorylation, and cytokine production in human keratinocytes. BMC Microbiol 11: 143.
28. Bottone EJ (2010) Bacillus cereus, a volatile human pathogen. Clin Microbiol Rev 23: 382–398.
29. Biotechnology Program under the Toxic Substances Control Act (TSCA) (2012) Bacillus subtilis Final Risk Assessment, USA. Available: http://www.epa.gov/biotech_rule/pubs/fra/fra009.htm. Accessed 2014 April 3.
30. Dixon TC, Meselson M, Guillemin J, Hanna PC (1999) Anthrax. N Engl J Med 341: 815–826.
31. Gelfand EW (2012) Intravenous immune globulin in autoimmune and inflammatory diseases. N Engl J Med 367: 2015–2025.
32. Schwab I, Nimmerjahn F (2013) Intravenous immunoglobulin therapy: how does IgG modulate the immune system? Nat Rev Immunol 13: 176–189.

Eur J Pediatr (2014) 173:1089–1093
DOI 10.1007/s00431-014-2296-4

ORIGINAL ARTICLE

# Evaluation of echogenicity of the heart in Kawasaki disease

**Hazumu Nagata · Kenichiro Yamamura · Kiyoshi Uike · Yasutaka Nakashima · Yuichiro Hirata · Eiji Morihana · Yumi Mizuno · Shiro Ishikawa · Toshiro Hara**

Received: 15 October 2013 / Revised: 27 February 2014 / Accepted: 4 March 2014 / Published online: 23 March 2014


**Abstract** Pathologic studies of the heart in patients with Kawasaki disease (KD) revealed vasculitis, valvulitis, myocarditis, and pericarditis. However, there have been no studies on the quantitative determination of multi-site echogenicity of the heart in KD patients. It is also undetermined whether the degree of echogenicity of each site of the heart in patients with KD might be related to the response to intravenous immunoglobulin (IVIG) treatment. In 81 KD patients and 30 control subjects, we prospectively analyzed echogenicity of the heart. Echogenicity was measured in four sites: coronary artery wall (CAW), mitral valve (MV), papillary muscle (PM), and ascending aortic wall (AAo wall) by the calibrated integrated backscatters (cIBs). The cIB values of all measurement sites at acute phase in KD patients were significantly higher than those in control subjects (KD patients vs control subjects; CAW, 19.8±6.2 dB vs 14.5±2.0 dB, $p<0.05$; MV, 23.3±5.3 dB vs 16.0±3.3 dB, $p<0.05$; PM, 22.4±5.1 dB vs 12.7±1.9 dB, $p<0.05$; AAo wall, 25.3±5.6 dB vs 18.3±3.4 dB,

Communicated by Jaan Toelen

**What is known?** It has been known that echogenicity of the coronary artery wall is increased at acute phase of KD. Some reports described the association between the echogenicity of the coronary artery wall and the formation of coronary artery lesions.

**What is new?** The present study has first demonstrated the increase of echogenicity of the heart in KD patients not only in coronary artery wall (CAW) but also in other portions of the heart (mitral valve papillary muscle and aortic wall). Echogenicity of CAW at acute phase in IVIG nonresponders was higher than that in IVIG responders.

**Electronic supplementary material** The online version of this article (doi:10.1007/s00431-014-2296-4) contains supplementary material, which is available to authorized users.

H. Nagata (✉) · K. Yamamura · K. Uike · Y. Nakashima · Y. Hirata · E. Morihana · T. Hara
Department of Pediatrics, Graduate School of Medical Sciences, Kyushu University, 3-1-1 Maidashi, Higashi-ku, Fukuoka City 812-8582, Japan
e-mail: dadan@pediatr.med.kyushu-u.ac.jp

K. Yamamura
e-mail: yamamura@pediatr.med.kyushu-u.ac.jp

K. Uike
e-mail: uike@pediatr.med.kyushu-u.ac.jp

Y. Nakashima
e-mail: ya-naka@pediatr.med.kyushu-u.ac.jp

Y. Hirata
e-mail: hrm_pfvc@gb3.so-net.ne.jp

E. Morihana
e-mail: morihana@pediatr.med.kyushu-u.ac.jp

T. Hara
e-mail: harat@pediatr.med.kyushu-u.ac.jp

Y. Mizuno · S. Ishikawa
Department of Pediatrics, Fukuoka Children's Hospital Medical Center, 3-1-1 Maidashi, Higashi-ku, Fukuoka City 812-8582, Japan

Y. Mizuno
e-mail: yumi-mi@mvc.biglobe.ne.jp

S. Ishikawa
e-mail: ishikawa.s@fcho.jp

$p<0.05$). The cIB values of CAW at the acute phase in IVIG nonresponders were significantly higher than those in responders. *Conclusion*: Echogenicity of the heart in KD patients at the acute phase increased not only in the coronary artery wall but also in other parts of the heart. Echogenicity of CAW might be helpful in determining the unresponsiveness of IVIG treatment.

**Keywords** Kawasaki disease · Echogenicity · Heart · Coronary artery lesion · Intravenous immunoglobulin

**Abbreviations**

| | |
|---|---|
| AAo | Wall ascending aortic wall |
| cIBs | Calibrated integrated backscatters |
| CAL | Coronary artery lesions |
| CAW | Coronary artery wall |
| IVIG | Intravenous immunoglobulin |
| KD | Kawasaki disease |
| MV | Mitral valve |
| PM | Papillary muscle |
| ROI | Region of interest |

## Introduction

Kawasaki disease (KD) is an acute febrile illness of childhood characterized by systemic vasculitis including coronary arteritis. The diagnosis of KD is confirmed by the presence of five of six criteria: fever, bilateral conjunctival injection, changes of the mucous membranes of the oropharynx, polymorphous rash, changes of the extremities, and cervical adenopathy [12]. Coronary artery lesions (CAL) are responsible for the morbidity and mortality of KD. In addition, cardiac dysfunction and mitral or aortic regurgitation are also observed in KD patients by echocardiography [5, 11, 16].

Pathologic studies of the heart in patients with KD revealed vasculitis, valvulitis, myocarditis, and pericarditis [3]. Echogenicity of the coronary artery wall is increased at acute phase of KD [12]. However, there has been no study on the multi-site echogenicity of the heart at the acute phase in KD patients. In the present study, we have performed a comprehensive and quantitative evaluation of echogenicity of the coronary artery wall, valve, myocardium, and aortic wall at acute phase and investigated whether echogenicity of each portion could be related to the response to intravenous immunoglobulin (IVIG) treatment or CAL formation in KD patients.

## Materials and methods

From October 2010 to November 2011, we enrolled 81 patients with KD who were admitted to the Kyusyu University Hospital, Fukuoka, Japan and the Fukuoka Children's Hospital and Medical Center for Infectious Diseases, Fukuoka, Japan, and 30 children of matched age who had been referred to the Kyushu University Hospital for the examination of ventricular septal defect ($n=22$), heart murmur ($n=5$), and atrial septal defect ($n=2$) and pulmonary hypertension ($n=1$) as a control group. The diagnosis of KD was based on the presence of five or six of principal clinical features (fever, bilateral conjunctival injection, changes of the mucous membranes of the oropharynx, polymorphous rash, changes of the extremities, and cervical adenopathy). All KD patients received oral aspirin (30 mg/kg/day) and 1–2 g/kg of IVIG as an initial treatment. IVIG nonresponder was defined as the patient who had persistent or recrudescent fever ≥24 h after completion of initial 2 g/kg IVIG. A diagnosis of CAL was made when the echocardiography showed an internal lumen diameter of ≥3 mm in a child <5 years old or ≥4 mm in a child ≥5 years old, if the internal diameter of the segment was at least 1.5 times as large as that of an adjacent segment or if the lumen appeared irregular [7].

Echocardiography was performed by five pediatric cardiologists. The images during three to five heartbeats were recorded on hard disk. Patients were prepared for echocardiography by administration of oral triclofos sodium or intravenous thiamylal sodium, if necessary. Based on the recorded data, echogenicity was measured at four sites: coronary artery wall (CAW), mitral valve (MV), papillary muscle (PM), and ascending aortic wall (AAo wall), and at four separate timings: acute phase (median, day 5; range, day 3–9), after defervescence (median, day 8; range, day 6–15), subacute phase (median, day 14; range, 10–19), and convalescent phase (median, day 30; range, 21–32) by single operator. The images of CAW and PM, and MV, and AAo wall were obtained using parasternal short-axis view and parasternal long-axis view, respectively. When the image was suitable for determining IB, at the end systolic (CAW, PM, AAo wall) or diastolic (MV) phase, the ellipsoidal region of interest (ROI) was placed in the left coronary artery wall (ROI, 1×4 mm), the anterolateral papillary muscle of left ventricle (ROI, 5×5 mm), the belly of the anterior mitral valve leaflet (ROI, 1×4 mm), and the wall of the ascending aorta (ROI, 2×4 mm). The value of echogenicity was evaluated by the calibrated integrated backscatters (cIBs) representing the difference of the integrated backscatters between the measurement site and the intracardiac blood pool adjacent to the target site [20] (Fig. S1). These values were obtained using Vivid 7 (GE Healthcare, Japan) equipped with 7-MHz probe (frame rate 87 frame/s). Analyses were performed using Q-Analysis software (GE Healthcare, Japan) by a single author.

There was good intraclass correlation coefficient at all measurement sites (intraobserver between two operators and interobserver: CAW 0.712 and 0.701, MV 0.761 and 0.740, PM 0.769 and 0.753, and AAo wall 0.710 and 0.691).

Statistical analyses were performed using JMP 8 (SAS Institute, Japan) and SPSS 17.0, and statistical significance was defined when a $p$ value was <0.05. An analysis of variance with repeated measures on one factor was used for the variables measured at the four timings: acute phase, after defervescence, subacute phase, and convalescent phase. All values of cIBs were reported as means±standard deviations in KD patients and control subjects. The clinical variables were reported as medians (ranges). The variables were compared between groups (KD patients vs control subjects, with vs without CAL and IVIG nonresponders vs responders) using Wilcoxon rank sum test.

We got ethics committee approval for this study in the Kyushu University and the Fukuoka Children's Hospital and Medical Center for Infectious Diseases. All parents of the patients provided informed consent before examination.

## Results

### Clinical characteristics of patients

The baseline profiles of KD patients and control subjects are shown in Table 1. The median age of KD patients was 24 months (range, 3–108 months). Forty-five of 81 KD patients were male, and 36 KD patients were female. The median day of illness at initial treatment was day 5 (range, 3–9). Fifty-six of the 81 KD patients received 1 g/kg IVIG treatment, and the 25 KD patients received 2 g/kg IVIG treatment as an initial treatment. Prednisolone was not given to any of the KD patients. As an additional treatment, IVIG ($n$=14), infliximab ($n$=9), high dose methylprednisolone ($n$=1), and urinastatin ($n$=14) were given when patients were refractory to IVIG. Fourteen of the 81 KD patients were IVIG nonresponders. Among the 14 IVIG nonresponders, 6 patients had CAL. Two of these patients showed persistent CAL. Sixteen of the KD patients had mild mitral valve regurgitation. There was no relation between the presence of mitral valve regurgitation and the degree of cIBs at mitral valve. Only one of the KD patients had mild aortic valve regurgitation and mild pericardial effusion.

**Table 1** The baseline profiles of KD patients and control subjects

| | KD ($n$=81) | Control subjects ($n$=30) |
|---|---|---|
| Age (month) | 24 (3–108) | 24 (4–120) |
| Male:female | 45:36 | 14:16 |
| Weight (kg) | 11.3 (6.2–36) | 12.0 (5.3–28) |
| Height (cm) | 84 (61–146) | 82 (63–138) |
| BSA ($m^2$) | 0.50 (0.31–1.23) | 0.51 (0.30–1.03) |
| Day of illness at initial treatment | 5 (3–9) | |

Values represent median (range)

*KD* Kawasaki disease, *n* number, *BSA* body surface area

### The comparison of the cIBS between KD patients and control subjects, and the change of the cIBs in the clinical course of KD patients

The cIBs of the KD patients at the acute phase were significantly higher than those of control subjects in all the measurement sites (CAW, 19.8±6.2 dB vs 14.6±2.2 dB, $p$<0.05; MV, 23.3±5.3 dB vs 16.1±3.6 dB, $p$<0.05; PM, 22.4±5.1 dB vs 12.2±3.4 dB, $p$<0.05; AAo wall, 25.3±5.6 dB vs 18.3±3.9 dB, $p$<0.05). The cIBs in the KD patients were decreased significantly at subacute phase in CAW, MV, PM, and AAo wall (CAW, 16.5±6.7 dB; MV, 20.0±12.1 dB; PM, 16.3±4.2 dB; AAo wall, 22.6±5.2 dB) (Fig. 1).

### The comparison of cIBS between nonresponders and responders to IVIG, and between patients with and without CAL

The cIBs at the acute phase in nonresponders were significantly higher than those in responders in CAW (nonresponders vs responders; CAW, 23.7±4.6 vs 18.8±6.2 dB $p$=0.0086) (Table 2). However, there was no significant difference between nonresponders and responders to IVIG in the cIBs of MV, PM, and AAo wall. The cIBs at the acute phase in the KD patients with CAL were significantly higher than those in the KD patients without CAL (with CAL, 24.5±4.5 dB; without CAL, 19.4±6.2 dB, $p$=0.0208). Among the nonresponders, the cIBs of CAW at the acute phase in KD patients with CAL tended to be higher than those without CAL (with CAL, 25.2±4.5 dB; without CAL, 22.8±4.7 dB, $p$=0.1917) (Table 2).

## Discussion

The present study has demonstrated that echogenicity of CAW, MV, PM, and AAo wall in KD patients at the acute phase were significantly higher than those of control subjects, and was decreased with time after IVIG treatment. Echogenicity of CAW at the acute phase of IVIG nonresponders was significantly higher than that of responders. Among nonresponders, echogenicity of CAW in KD patients with CAL tended to be higher than those without CAL.

The backscatter method has been used for many studies in the field of internal medicine, for examples myocarditis [9, 14], atherosclerosis [19], Takayasu's arteritis [15], and mitral valve disease [18]. These authors discussed that the changes of the degree of backscatter were caused by fibrosis, calcification, and edematous change of tissues. Although this

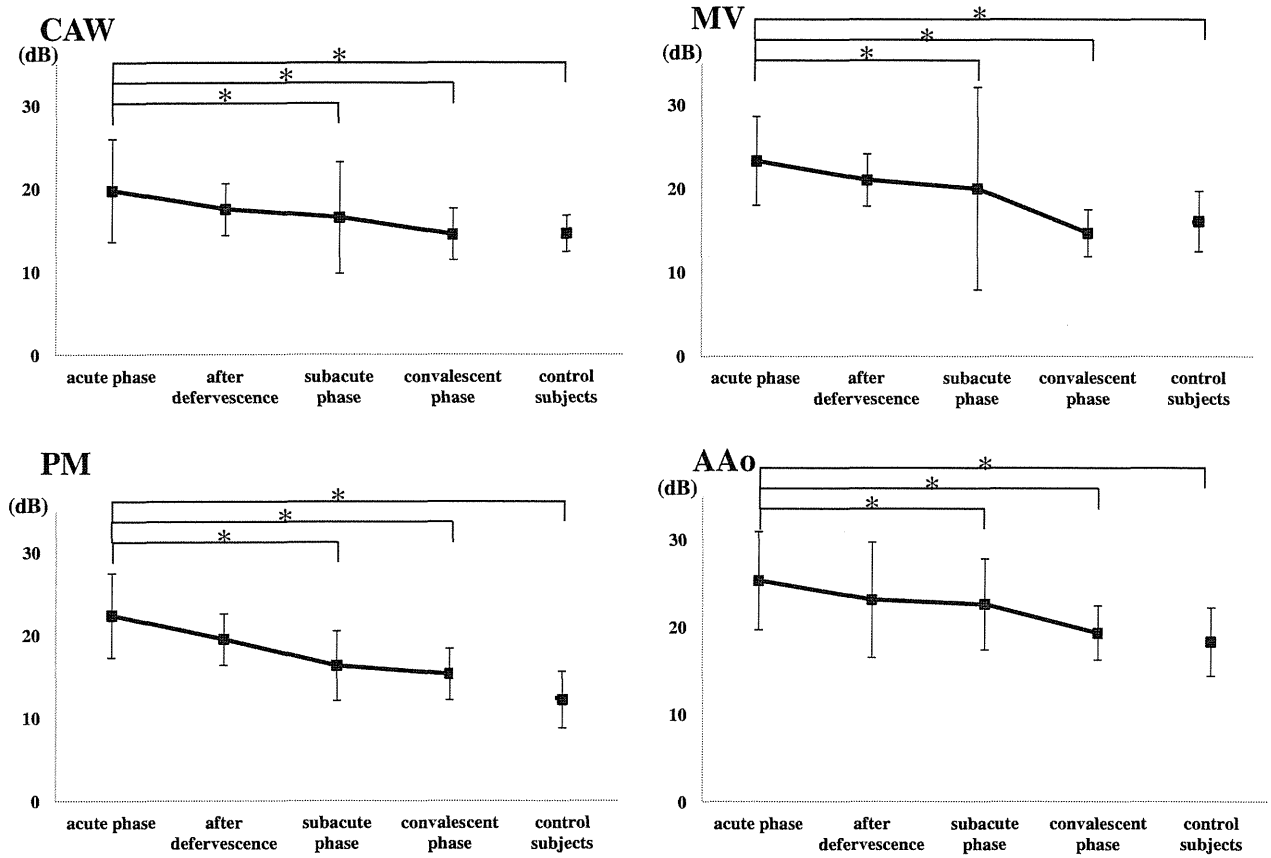


**Fig. 1** The comparison of the cIBS between KD patients and control subjects and the change of the cIBs in the clinical course of KD patients. The cIBs in the KD patients were decreased significantly at subacute phase in CAW, MV, PM, and AAo wall. *cIBs* calibrated integrated backscatter, *KD* Kawasaki disease, *CAW* coronary artery wall, *MV* mitral valve, *PM* papillary muscle, *AAo wall* ascending aortic wall

backscatter method is not popular in children, it is simple, easy, and noninvasive for the evaluation of echogenicity of the heart. Not only cardiologists but also general pediatricians could evaluate echogenicity by this method.

Generally, the histological alterations such as edema and cell infiltration associated with inflammation of the tissues change its acoustic properties [9]. KD is a systemic vasculitis of relatively large muscular arteries. At the early stage in KD, coronary vasculitis, valvulitis, myocarditis, and pericarditis were actually observed by pathological examinations.

**Table 2** The comparison of cIBs between IVIG responders and nonresponders and between patients with and without CAL at CAW

| Responders | Nonresponders | | *p* value |
|---|---|---|---|
| 18.8±6.2 | 23.7±4.6 | | 0.0086 |
| | CAL (+) | CAL (−) | 0.1917 |
| | 25.2±4.5 | 22.8±4.7 | |

Values represent mean±standard deviation

*cIBs* calibrated integrated backscatters, *IVIG* intravenous immunoglobulin, *CAW* coronary artery wall

Furthermore, patients with KD at the acute phase often show clinical or subclinical myocarditis and valvulitis [4, 11, 17]. The present study has suggested that the edematous change and cell infiltration in various portions of the heart as well as in the coronary artery wall will develop at the acute phase in most KD patients and improve gradually. This is consistent with our novel murine KD model, in which coronary arteritis, valvulitis, and aortic inflammation are observed at acute phase by oral administration of a synthetic innate immune receptor ligand, FK565, with a molecular weight of 502.6 Da [13].

There are only a few previous reports describing echogenicity of coronary arteries and myocardium in KD by the backscatter method, and the association between echogenicity and IVIG unresponsiveness has not been investigated. According to the report of Abe et. al., the magnitude of cIBs of CAW after IVIG treatment may be useful for prediction of CAL formation [1]. Leonardi et. al. reported that the ultrasound tissue characterization by the integrated backscatter of the patients years after an acute episode of KD differed from that of control subjects [8]. On the other hand, echogenicity of pericoronary tissue of the acute phase was not associated with the diameter of coronary artery, and was not

significantly higher than that of convalescent phase or control groups in another report by Yu et.al. [20]. However, in the study of Yu et.al, the analysis of cIBS was performed by a different method from the present study. The clinical phenotype of KD is different from population to population. These factors could explain the differences between the results of our studies and the study from Yu et.al. The numbers of patients of these reports were smaller than that of the present study. There have been no comprehensive studies on echogenicity of the portions other than CAW of the heart. The present study suggested the similar changes of the tissue took place in various portions other than CAW of the heart, and the degrees of echogenicity of CAW in KD patients at the acute phase might be associated with the unresponsiveness of IVIG treatment.

Several studies presented a scoring method or risk factors to evaluate the severity of KD and to predict the IVIG unresponsiveness and occurrence of CAL with a certain level of accuracy [2, 6, 10]. However, no previous studies took into account the echogenicity of the heart. The evaluation of echogenicity of CAW might be helpful for the further improvement of the accuracy to predict the unresponsiveness of IVIG treatment.

However, there were several limitations in the present study. First, the image of echocardiography was recorded by several examiners. A single examiner blinded to the patients' information might be better in a future study. Second, although we performed echocardiography under standardized conditions and used IB values relative to the background ROI, we did not consider the influence of the patients' build including thoracic thickness. Further study to evaluate the particular effect of patients' build would add more information to the present study. Third, our study did not include the disease control. We should investigate the echogenicity of the heart in the patients with common febrile diseases in a future study. This study is not blind.

In conclusion, the present study has first demonstrated the increase of echogenicity of the heart in KD patients not only in CAW but also in other portions of the heart. Echogenicity of CAW might be helpful in predicting the unresponsiveness of IVIG treatment.

**Conflict of interest** Authors have nothing to disclose with regard to commercial support.

## References

1. Abe O, Karasawa K, Hirano M, Miyashita M, Taniguchi K, Ayusawa M, Sumitomo N, Okada T, Harada K, Mugishima H (2010) Quantitative evaluation of coronary artery wall echogenicity by integrated backscatter analysis in Kawasaki disease. J Am Soc Echocardiogr 23:938–942
2. Egami K, Muta H, Ishii M, Suda K, Sugahara Y, Iemura M, Matsuishi T (2006) Prediction of resistance to intravenous immunoglobulin treatment in patients with Kawasaki disease. J Pediatr 149: 237–240
3. Fujiwara H, Hamashima Y (1978) Pathology of the heart in Kawasaki disease. Pediatrics 61:100–107
4. Harada M, Yokouchi Y, Oharaseki T, Matsui K, Tobayama H, Tanaka N, Akimoto K, Takahashi K, Kishiro M, Shimizu T (2012) Histopathological characteristics of myocarditis in acute-phase Kawasaki disease. Histopathology 61:1156–1167
5. Kato H, Sugimura T, Akagi T, Sato N, Hashino K, Maeno Y, Kazue T, Eto G, Yamakawa R (1996) Long-term consequences of Kawasaki disease. A 10- to 21-year follow-up study of 594 patients. Circulation 94:1379–1385
6. Kim T, Choi W, Woo CW, Choi B, Lee J, Lee K, Son C, Lee J (2007) Predictive risk factors for coronary artery abnormalities in Kawasaki disease. Eur J Pediatr 166:565–571
7. Kobayashi T, Inoue Y, Takeuchi K, Okada Y, Tamura K, Tomomasa T, Morikawa A (2006) Prediction of intravenous immunoglobulin unresponsiveness in patients with Kawasaki disease. Circulation 113: 2606–2612
8. Leonardi B, Giglio V, Sanders SP, Pasceri V, De Zorzi A (2010) Ultrasound tissue characterization of the myocardium in patients after Kawasaki disease. Pediatr Cardiol 31:766–772
9. Lieback E, Hardouin I, Meyer R, Bellach J, Hetzer R (1996) Clinical value of echocardiographic tissue characterization in the diagnosis of myocarditis. Eur Heart J 17:135–142
10. Muta H, Ishii M, Furui J, Nakamura Y, Matsuishi T (2006) Risk factors associated with the need for additional intravenous gammaglobulin therapy for Kawasaki disease. Acta Paediatr 95:189–193
11. Nakano H, Nojima K, Saito A, Ueda K (1985) High incidence of aortic regurgitation following Kawasaki disease. J Pediatr 107:59–63
12. Newburger JW, Takahashi M, Gerber MA, Gewitz MH, Tani LY, Burns JC, Shulman ST, Bolger AF, Ferrieri P, Baltimore RS, Wilson WR, Baddour LM, Levison ME, Pallasch TJ, Falace DA, Taubert KA (2004) Diagnosis, treatment, and long-term management of Kawasaki disease: a statement for health professionals from the Committee on Rheumatic Fever, Endocarditis and Kawasaki Disease, Council on Cardiovascular Disease in the Young, American Heart Association. Circulation 110:2747–2771
13. Nishio H, Kanno S, Onoyama S, Ikeda K, Tanaka T, Kusuhara K, Fujimoto Y, Fukase K, Sueishi K, Hara T (2011) Nod1 ligands induce site-specific vascular inflammation. Arterioscler Thromb Vasc Biol 31:1093–1099
14. Omi W, Nagai H, Takata S, Yuasa T, Sakagami S, Kobayashi K (2002) Ultrasonic tissue characterization in acute myocarditis: a case report. Circ J 66:416–418
15. Park SH, Chung JW, Lee JW, Han MH, Park JH (2001) Carotid artery involvement in Takayasu's arteritis: evaluation of the activity by ultrasonography. J Ultrasound Med 20:371–378
16. Takeuchi D, Saji T, Takatsuki S, Fujiwara M (2007) Abnormal tissue doppler images are associated with elevated plasma brain natriuretic peptide and increased oxidative stress in acute Kawasaki disease. Circ J 71:357–362
17. Tomita H, Sawada Y, Higashidate Y, Chiba S, Ito S, Kogasaka R (1990) Mitral regurgitation with gross deformity of a mitral leaflet due to Kawasaki disease. Pediatr Cardiol 11:153–155
18. Warsame TA, Keen OE, Mookadam F, Chaliki HP (2009) Liquefaction necrosis of calcified mitral annulus. Echocardiography 26:1082–1083
19. Weber HS, Myers JL (1994) Maternal collagen vascular disease associated with fetal heart block and degenerative changes of the atrioventricular valves. Pediatr Cardiol 15:204–206
20. Yu JJ, Jang WS, Ko HK, Han MK, Kim YH, Ko JK, Park IS (2011) Perivascular brightness of coronary arteries in Kawasaki disease. J Pediatr 159(454–457):e1

impinge on the *Bcl6* locus where STAT5 can outcompete STAT3 on shared binding sites to repress *Bcl6* transcription (Figure 1). Rather than opening closed doors in $CD4^+$ T cell differentiation, type I interferons' interference in Tfh deviates differentiation toward Th1 cells, if STAT3-activating signals are missing. Besides the known adjuvant effect of type I interferon on non-T cells, the present study demonstrates a crucial importance for balanced cytokine signals to enable efficient Tfh cell differentiation in vaccination strategies. At the same time, it highlights the potential of STAT3 as a target to treat autoimmune diseases that involve Tfh cells.

REFERENCES

Choi, Y.S., Eto, D., Yang, J.A., Lao, C., and Crotty, S. (2013). J. Immunol. *190*, 3049–3053.

Hegazy, A.N., Peine, M., Helmstetter, C., Panse, I., Fröhlich, A., Bergthaler, A., Flatz, L., Pinschewer, D.D., Radbruch, A., and Löhning, M. (2010). Immunity *32*, 116–128.

Johnston, R.J., Choi, Y.S., Diamond, J.A., Yang, J.A., and Crotty, S. (2012). J. Exp. Med. *209*, 243–250.

Lee, S.K., Silva, D.G., Martin, J.L., Pratama, A., Hu, X., Chang, P.P., Walters, G., and Vinuesa, C.G. (2012). Immunity *37*, 880–892.

Lüthje, K., Kallies, A., Shimohakamada, Y., Belz, G.T., Light, A., Tarlinton, D.M., and Nutt, S.L. (2012). Nat. Immunol. *13*, 491–498.

Nakayamada, S., Poholek, A.C., Lu, K.T., Takahashi, H., Kato, M., Iwata, S., Hirahara, K., Cannons, J.L., Schwartzberg, P.L., Vahedi, G., et al. (2014). Journal of Immunology, 1300675. Published online January 31, 2014. http://dx.doi.org/10.4049/jimmunol.1300675.

Nurieva, R.I., Podd, A., Chen, Y., Alekseev, A.M., Yu, M., Qi, X., Huang, H., Wen, R., Wang, J., Li, H.S., et al. (2012). J. Biol. Chem. *287*, 11234–11239.

Oestreich, K.J., Mohn, S.E., and Weinmann, A.S. (2012). Nat. Immunol. *13*, 405–411.

Ray, J.P., Marshall, H.D., Laidlaw, B.J., Staron, M.M., Kaech, S.M., and Craft, J. (2014). Immunity *40*, this issue, 367–377.

Yamane, H., and Paul, W.E. (2012). Nat. Immunol. *13*, 1037–1044.

# Clec12a: Quieting the Dead

**Sho Yamasaki**[1,*]
[1]Division of Molecular Immunology, Research Center for Infectious Diseases, Medical Institute of Bioregulation, Kyushu University, 3-1-1 Maidashi Higashiku, Fukuoka 812-8582, Japan
*Correspondence: yamasaki@bioreg.kyushu-u.ac.jp
http://dx.doi.org/10.1016/j.immuni.2014.03.001

Immune activation as a result of the recognition of damage-associated molecular patterns needs to be controlled. In this issue of *Immunity*, Neumann et al. (2014) demonstrates that Clec12a is a receptor for dead cells through the recognition of uric acid crystals and contributes to the dampening of the responses.

C-type lectin receptors (CLRs) are pattern-recognition receptors (PRRs) that recognize microbial pathogen-associated molecular patterns (PAMPs), which leads to the induction of host immune responses against many pathogens (Robinson et al., 2006). In addition to acting as PRRs for PAMPs, some CLRs also function as receptors for damage-associated molecular patterns (DAMPs), which are exposed or released upon cell death by noninfectious insults such as tissue injury, ischemia, and infarction. For example, Lox-1 and MGL-1 are CLRs known to recognize dead cells and are likely to act as phagocytic receptors for dead cells (Robinson et al., 2006). Some CLRs coupled with immunoreceptor tyrosine-based activation motif (ITAM) or hemITAM (hemi-immunoreceptor tyrosine-based activation motif), such as Mincle (Clec4e) and DNGR-1 (Clec9a), have also been shown to recognize dead cells (Sancho et al., 2009; Yamasaki et al., 2008). These CLRs sense nonhomeostatic cell death and thereby induce inflammation or promotion of antigen presentation. These immune responses against "damaged self" are thought to be beneficial to maintain homeostasis of the organisms. In contrast, the "anti-self" responses should be immediately terminated to prevent tissue damage or autoimmunity caused by prolonged halmful immune reaction against self. To date, however, negative regulatory CLRs for dead cells have never been identified. Several CLRs possesses immunoreceptor tyrosine-based inhibitory motif (ITIM) within their own cytoplasmic tails. Upon receptor engagement, tyrosine residues within ITIM are phosphorylated and thus provide docking sites for cytosolic negative regulatory proteins such as SHP-1, SHP-2, or SHIP. In T cells, ITIM-containing costimulatory inhibitory receptors CTLA-4 and PD-1 play critical roles in terminating activatory signals delivered through ITAM-containing T cell receptor (TCR) complexes in order to prevent autoimmunity. Likewise, it is possible that unknown inhibitory CLR(s) contribute to the negative regulation of immune responses against damaged self.

Clec12a (also called myeloid inhibitory C-type lectin-like receptor, MICL) was originally described as an ITIM-containing inhibitory CLR expressed by human granulocytes and monocytes (Marshall et al., 2006). It was suggested that Clec12a recognizes some endogenous ligands as soluble Clec12a could bind to single-cell suspensions isolated from various murine tissues (Pyz et al., 2008). In this issue of *Immunity*, Neumann et al. (2014) identified Clec12a as an inhibitory CLR for dead

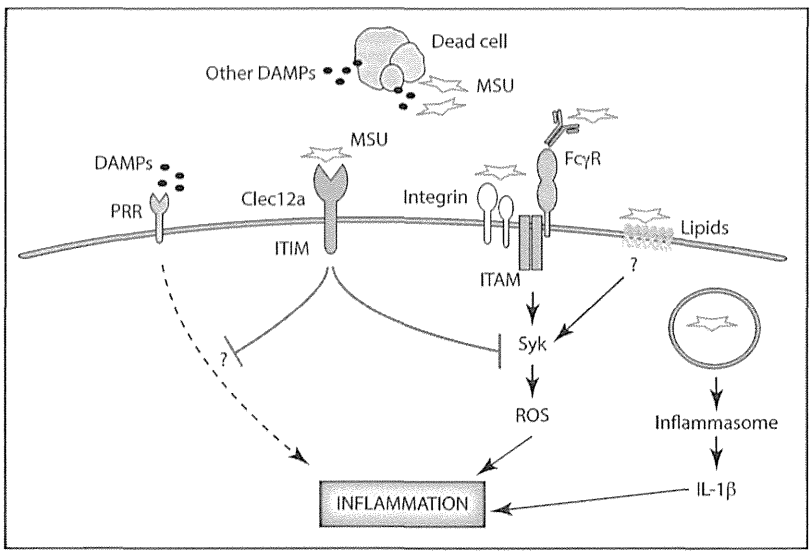


**Figure 1. Schematic Representation of the Negative Regulation of Immune Responses against Damaged Self by Clec12a**

Excessive or deregulated cell death results in the release of DAMPs. Among them, uric acid forms MSU crystal by contacting extracellular sodium ions. MSU can be opsonized with antibodies and thus binds to cell surface Fc receptors coupled with ITAM-containing FcRγ chain. MSU crystals activate myeloid cells through CD11b and/or FcγRIII and membrane lipid in a Syk-dependent manner, which leads to ROS production. Clec12a is likely to inhibit Syk activation presumably through recruiting PTPase to the phosphorylated ITIM. MSU crystal also induces IL-1β production via inflammasome. This inflamasome-dependent pathway appears to be resistant to Clec12a-mediated negative regulation. The effect of Clec12a on other receptors for DAMPs, such as TLRs and CLRs, remains unclear.

cells. The authors found that mouse and human Clec12a recognizes dead cells derived from 293T cells or thymocytes by using Clec12a-immunoglobulin (Ig) fusion protein and reporter cells expressing Clec12a-CD3ζ chimera. Clec12a also recognized dead cells from meshed murine organs. To further characterize the ligand components, the authors treated killed kidney cells with DNase, RNase, trypsin, and inhibitor of uric acid synthesis. Among these, only uric acid inhibitor could eliminate Clec12a-Ig binding to dead cells. Uric acid is soluble within healthy cells, but when it is contact with extracellular sodium ions upon cell death, uric acid forms monosodium urate (MSU) crystal. Neumann et al. demonstrated that MSU is a direct ligand for Clec12a.

Deposition of MSU crystal causes a common inflammatory arthritis called gout. MSU is a DAMP associated with cell death (Shi et al., 2003). However, the molecular mechanism underlying the "crystal-induced" inflammatory responses has remained elusive. It has been thought that MSU is opsonized with antibodies, which might trigger Fc receptors coupled with FcRγ chain (Shi et al., 2010). In addition, inflammatory MSU induces Syk activation through the engagement of FcγRIII and CD11b in neutrophils (Barabé et al., 1998). It is also proposed that direct membrane binding of MSU results in cell-surface lipid sorting and Syk activation in an ITAM-independent fasion (Shi et al., 2010). In contrast, Martinon et al. reported that MSU crystals activate NRLP3 inflammasome, followed by the secretion of active (mature) interleukin-1β (IL-1β) through caspase-1 activation (Martinon et al., 2006). To maintain tissue homestasis by preventing excessive "detrimental" inflammation, these immune responses against MSU need to be strictly regulated.

To gain insight into the physiological relevance of this finding, Neumann et al. generated Clec12a-deficient mice and investigated neutrophil activation in response to MSU. As previously reported, MSU induced reactive oxygen species (ROS) production in a Syk-dependent manner, and it was substantially increased in the absence of Clec12a. Thus, Clec12a is likely to downmodulate MSU response through the inhibition of Syk activity, although this was not addressed in this study. This phenomenon was also confirmed by in vivo experiments in which MSU crystal was injected into the peritoneum of mice. MSU-induced neutrophil infiltration to peritoneal cavity was augmented in *Clec12a*$^{-/-}$ mice. In contrast, ROS production induced by irrelevant Dectin-1 ligand was not enhanced in *Clec12a*$^{-/-}$ mice, implying that coengagement with activating receptor might be required for Clec12a to exert its inhibitory effects. It would be intriguing to test whether antibody-mediated crosslinking of Clec12a could suppress activation of immune cells induced by PRRs for other DAMPs. Finally, Neumann et al. investigated noninfectious inflammation induced by dead cells in vivo. Infiltration of neutrophil in response to dead cells was significantly enhanced in the absence of Clec12a. Thus, Clec12a appears to be an inhibitory CLR that senses dead cells to control sterile inflammation (Figure 1).

Several interesting questions remain to be solved. Currently, it is unclear how Clec12a can recognize MSU. The nature of the MSU crystals such as "ruggedness" has been thought to be linked to the different inflammatory potential (Shi et al., 2010). Does Clec12a discriminate different "shape" or "size" of the crystals? Further understanding of the binding mode will be achieved by the structural analyses of the crystallized Clec12a-MSU complex. Alternatively, it is conceivable that other components such as opsonizing proteins, carbohydrates, lipids, or nucleic acids might modulate the interaction of MSU with Clec12a. In addition, because Clec12a possesses ITIM within the cytoplasmic tail, some PTPases are likely to mediate the negative regulatory role of Clec12a. More detailed studies will clarify the cytosolic inhibitory signaling pathways underlying the negative regulation.

It is still an open question whether MSU is the sole ligand for Clec12a. Other endogenous ligand(s) derived from dead cells might also contribute to attenuate sterile inflammation through the use of Clec12a. In contrast, it is reported that MSU is recognized by the inflammasome, which leads to the production of proinflammatory cytokine IL-1β. Given that this pathway appeared to be resistant to

Clec12a (Neumann et al., 2014), other intracellular sensor(s) for MSU might be operating in the negative regulation of inflammasome-caspase-1 axis. MSU is characterized as an endogenous adjuvant that promotes acquired immune responses (Shi et al., 2003). Because Clec12a is also expressed in dendritic cells, it would be valuable to examine whether Clec12a can inhibit T cell-mediated immunity by regulating antigen-presenting cells.

These findings shed light on ITIM-containing CLRs as important negative regulators that potentially dampen immune responses against DAMPs. The development of selective agonist for Clec12a is of interest in the treatment of a variety of inflammatory diseases associated with high systemic uric acid levels, such as arthritis, atherosclerosis, cardiovascular diseases, and type 2 diabetes.

REFERENCES

Barabé, F., Gilbert, C., Liao, N., Bourgoin, S.G., and Naccache, P.H. (1998). FASEB J. *12*, 209–220.

Marshall, A.S., Willment, J.A., Pyz, E., Dennehy, K.M., Reid, D.M., Dri, P., Gordon, S., Wong, S.Y., and Brown, G.D. (2006). Eur. J. Immunol. *36*, 2159–2169.

Martinon, F., Pétrilli, V., Mayor, A., Tardivel, A., and Tschopp, J. (2006). Nature *440*, 237–241.

Neumann, K., Castiñeiras-Vilariño, M., Höckendorf, U., Hannesschläger, N., Lemeer, S., Kupka, K., Meyermann, S., Lech, M., Anders, H.-J., Kuster, B., et al. (2014). Immunity *40*, this issue, 389–399.

Pyz, E., Huysamen, C., Marshall, A.S., Gordon, S., Taylor, P.R., and Brown, G.D. (2008). Eur. J. Immunol. *38*, 1157–1163.

Robinson, M.J., Sancho, D., Slack, E.C., LeibundGut-Landmann, S., and Reis e Sousa, C. (2006). Nat. Immunol. *7*, 1258–1265.

Sancho, D., Joffre, O.P., Keller, A.M., Rogers, N.C., Martínez, D., Hernanz-Falcón, P., Rosewell, I., and Reis e Sousa, C. (2009). Nature *458*, 899–903.

Shi, Y., Evans, J.E., and Rock, K.L. (2003). Nature *425*, 516–521.

Shi, Y., Mucsi, A.D., and Ng, G. (2010). Immunol. Rev. *233*, 203–217.

Yamasaki, S., Ishikawa, E., Sakuma, M., Hara, H., Ogata, K., and Saito, T. (2008). Nat. Immunol. *9*, 1179–1188.

# Dendritic Cells Decide CD8$^+$ T Cell Fate

**Allan McI. Mowat**[1,*]
[1]Centre for Immunobiology, Institute of Infection, Immunity and Inflammation, University of Glasgow, Sir Graeme Davies Building, Glasgow G12 8TA, Scotland, UK
*Correspondence: allan.mowat@glasgow.ac.uk
http://dx.doi.org/10.1016/j.immuni.2014.02.011

In this issue of *Immunity*, Kim et al. (2014) propose that CD103$^+$ DCs in mouse lung selectively generate effector CD8$^+$ T cells by binding the alarmin HMGB1 via CD24 and presenting it to RAGE$^+$ T cells.

Whether the same dendritic cell (DC) can prime all kinds of T cells or whether individual T cell populations require antigen to be presented by separate populations of DCs has long been an issue in immunology. Addressing these questions is important not just for understanding the basic tenets of immune function, but also for identifying which DC might be useful to target in designing vaccines or tailoring immunotherapy.

In this issue of *Immunity*, Kim et al. (2014) show that separate DC subsets in the influenza A virus (IAV)-infected lung may play distinct roles in driving local effector or memory CD8$^+$ T cell responses. Whereas CD103$^+$CD11b$^-$ DCs generate short-lived CD8$^+$ effector T cells that home to the lung and confer protective immunity, CD103$^-$CD11b$^+$ DCs drive the generation of "central memory" CD8$^+$ T cells that reside in secondary lymphoid organs for long periods after infection. The CD103$^+$ DCs that drive effector CD8$^+$ T cell differentiation express very high amounts of CD24; blockade and overexpression of CD24 show that the amount of CD24 controls whether effector or memory CD8$^+$ T cells are generated by the same virus challenge. It is proposed that CD24 acts by allowing CD103$^+$ DCs to decorate their surface with high mobility group box 1 (HMGB1) protein, a histone-related protein that acts as a damage-associated molecular pattern (DAMP) molecule when released from dying cells in the lung (Ullah et al., 2014) and whose receptor, RAGE (receptor for advanced glycation endproducts), can act as a costimulatory signal in T cells (Moser et al., 2007). Kim et al. (2014) then demonstrate that blocking the interaction between CD24, HMGB1, and RAGE markedly inhibits priming of CD8$^+$ T cells in vivo and in vitro. The authors conclude that CD103$^+$ DCs can thus provide the strong signal needed to generate effector CD8$^+$ T cells (Figure 1). It is known that efficient T cell priming and high amounts of IL-2 production favor the differentiation of short-lived effector versus long-lived memory CD8$^+$ T cells (Kalia et al., 2010). This has usually been assumed to reflect differences in the TCR-pMHC interaction. The work of Kim et al. (2014) now suggests that such decisions are not controlled simply via the TCR, but involve additional non-antigen-specific costimulatory processes such as the CD24-HMGB1-RAGE axis.

The current work may also help explain apparent contradictions in the literature about how CD103$^+$ and CD11b$^+$ DCs may divide their labor in CD8$^+$ T cell responses in the lung. Although a consensus has subsequently arisen that migratory CD103$^+$ DCs play the dominant role in priming CD8$^+$ T cell responses in the MedLN, a role for migratory CD11b$^+$ DCs has also long been suspected

CellPress

Immunity
Article

# Dectin-2 Is a Direct Receptor for Mannose-Capped Lipoarabinomannan of Mycobacteria

Akiko Yonekawa,[1,2,9] Shinobu Saijo,[3,4,9] Yoshihiko Hoshino,[5] Yasunobu Miyake,[1] Eri Ishikawa,[1] Maho Suzukawa,[6] Hiromasa Inoue,[7] Masato Tanaka,[8] Mitsutoshi Yoneyama,[3] Masatsugu Oh-hora,[1,4] Koichi Akashi,[2] and Sho Yamasaki[1,3,*]
[1]Division of Molecular Immunology, Medical Institute of Bioregulation
[2]Department of Medicine and Biosystemic Science, Graduate School of Medical Sciences
Kyushu University, Fukuoka 812-8582, Japan
[3]Division of Molecular Immunology, Medical Mycology Research Center, Chiba University, Chiba 260-8673, Japan
[4]PRESTO, Japan Science and Technology Agency (JST), Saitama 332-0012, Japan
[5]Leprosy Research Center, National Institute of Infectious Diseases, Tokyo 189-0002, Japan
[6]Center for Pulmonary Diseases, National Hospital Organization, Tokyo National Hospital, Tokyo 204-8585, Japan
[7]Department of Pulmonary Medicine, Graduate School of Medical and Dental Sciences, Kagoshima University, Kagoshima 890-8544, Japan
[8]Laboratory for Immune Regulation, School of Life Sciences, Tokyo University of Pharmacy and Life Sciences, Tokyo 192-0392, Japan
[9]Co-first author
*Correspondence: yamasaki@bioreg.kyushu-u.ac.jp
http://dx.doi.org/10.1016/j.immuni.2014.08.005

## SUMMARY

Mycobacteria possess various immunomodulatory molecules on the cell wall. Mannose-capped lipoarabinomannan (Man-LAM), a major lipoglycan of *Mycobacterium tuberculosis*, has long been known to have both inhibitory and stimulatory effects on host immunity. However, the direct Man-LAM receptor that explains its pleiotropic activities has not been clearly identified. Here, we report that a C-type lectin receptor Dectin-2 (gene symbol *Clec4n*) is a direct receptor for Man-LAM. Man-LAM activated bone-marrow-derived dendritic cells (BMDCs) to produce pro- and anti-inflammatory cytokines, whereas it was completely abrogated in *Clec4n*$^{-/-}$ BMDCs. Man-LAM promoted antigen-specific T cell responses through Dectin-2 on DCs. Furthermore, Man-LAM induced experimental autoimmune encephalitis (EAE) as an adjuvant in mice, whereas *Clec4n*$^{-/-}$ mice were resistant. Upon mycobacterial infection, *Clec4n*$^{-/-}$ mice showed augmented lung pathology. These results demonstrate that Dectin-2 contributes to host immunity against mycobacterial infection through the recognition of Man-LAM.

## INTRODUCTION

Mycobacteria possess various cell wall components that influence host immune responses, such as trehalose-6,6′-dimycolate (TDM), mycolate, phosphatidyl-*myo*-inositol mannosides (PIMs), lipomannnan (LM), and lipoarabinomannan (LAM). LAM is a major lipoglycan and important virulence factor of mycobacteria (Mishra et al., 2011), enabling mycobacteria to infect host organisms and survive within host cells. Ethambutol, an inhibitor of LAM synthesis, is widely used as an antimycobacterial drug (Belanger et al., 1996). LAM consists of four components: a mannosyl-phosphatidyl-*myo*-inositol (MPI) anchor, a mannose backbone, an arabinan domain, and capping moieties. The capping moieties located at the terminal extremity of the arabinan domain differ among mycobacterial species, such as mannose-capped LAM (Man-LAM), phosphoinositol-capped LAM (PI-LAM), and noncapped LAM (Ara-LAM). Among them, Man-LAM has been intensively studied because it exerts pleiotropic effects on host immunity (Mishra et al., 2011).

Pathogenic species, including *Mycobacterium tuberculosis*, possess Man-LAM, which has been shown to suppress host immune system (Briken et al., 2004) and phagosome-lysosome fusion (Fratti et al., 2003). Although various inhibitory mechanisms have been proposed thus far, one of the key events is the production of immunosuppressive cytokine interleukin-10 (IL-10). On the other hand, Man-LAM also potentiates immunostimulatory responses, such as nitric oxide release and secretion of proinflammatory cytokines (Chan et al., 2001; Gringhuis et al., 2009; Mazurek et al., 2012).

C-type lectin receptors (CLRs) have been recently identified as pattern recognition receptors (PRRs) for a wide variety of pathogens. A member of CLRs, dendritic-cell (DC)-specific intercellular adhesion molecule-3 grabbing nonintegrin (DC-SIGN, also called CD209) and its putative murine homologs SIGN-related 1 (SIGNR1, also called CD209b) and SIGNR3 (CD209d) are reported to recognize Man-LAM and mediate its immunosuppressive activities (Geijtenbeek et al., 2003; Schlesinger et al., 1994; Tailleux et al., 2003). Macrophage mannose receptor (MMR, also called CD206) is also a candidate for inhibitory receptor for LAM, because it delivers a negative signal to attenuate DC activation (Nigou et al., 2001). In addition to these reports regarding inhibitory functions, engagement of SIGNR3 by Man-LAM also induces the secretion of IL-6 and tumor necrosis factor (TNF) in macrophages transfected with SIGNR3 (Tanne et al., 2009). Moreover, the scavenger receptor CD36 enhances the stimulatory activity of Man-LAM leading to TNF release in lipopolysaccharide (LPS)-stimulated macrophage cell line (Józefowski et al., 2011). Although many proteins have been proposed as a receptor for Man-LAM, none of these receptors fully explain its divergent functions, both stimulatory and inhibitory effects,

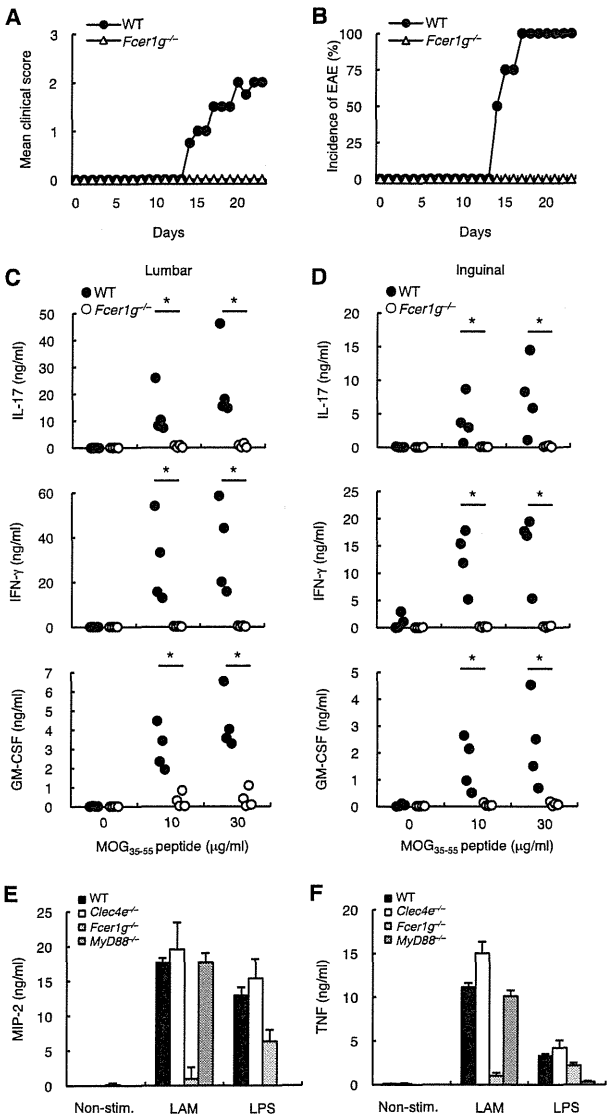


**Figure 1. LAM Induces EAE through FcRγ Axis**

(A and B) WT (n = 4) and *Fcer1g*$^{-/-}$ (n = 4) mice were immunized with $MOG_{35-55}$ peptide in IFA containing LAM (500 μg), followed by i.p. injection of PT (500 ng) (day 1, 2, and 3). The disease severity of each mouse was scored, and mean clinical score (A) and disease incidence (B) at the indicated times were plotted.

(C and D) Lumbar (C) and inguinal (D) lymph nodes were collected at 23 days after immunization. Lymph node cells were stimulated with $MOG_{35-55}$ peptide for 4 days. Concentrations of IL-17, IFN-γ, and GM-CSF were determined with ELISA.

(E and F) BMDCs obtained from WT, *Clec4e*$^{-/-}$, *Fcer1g*$^{-/-}$, or *MyD88*$^{-/-}$ mice were stimulated with plate-coated LAM (0.3 μg/well) or LPS (10 ng/ml) for 48 hr. The concentrations of MIP-2 (E) and TNF (F) were measured using ELISA.

(A–D) Data are representative of two separate experiments.

(E and F) All data are presented as the means ± SD of triplicate and are representative of three separate experiments.

See also Figure S1.

suggesting the possibility that unidentified molecules act as receptors for Man-LAM.

We recently demonstrated that CLRs Mincle (gene symbol *Clec4e*) and MCL (gene symbol *Clec4d*) are Fc receptor γ chain (FcRγ, gene symbol *Fcer1g*)-coupled activating receptors for mycobacterial glycolipids (Ishikawa et al., 2009; Miyake et al., 2013). Another CLR, DC-associated C-type lectin-2 (Dectin-2, gene symbol *Clec4n*), is located adjacent to Mincle and MCL within the gene cluster on chromosome 6. Dectin-2 is an FcRγ-coupled CLR (Sato et al., 2006) that recognizes *Candida albicans* hyphae to mediate host defense against the fungus (Robinson et al., 2009; Saijo et al., 2010). Dectin-2 and MCL seem to have arisen by gene duplication from Mincle after placentalia and are well conserved among species (Miyake et al., 2013). These findings imply that these CLRs within the gene cluster might have evolved as "mycobacterial receptors" and that Dectin-2 might also recognize mycobacteria.

In this study, we show that Dectin-2 is a direct receptor for Man-LAM. Man-LAM recognition by Dectin-2 induced the production of both pro- and anti-inflammatory cytokines in DCs. Man-LAM potently promoted T-cell-mediated acquired immunity as an adjuvant without causing detrimental inflammation. We further demonstrate, through Dectin-2-deficient mice, that Dectin-2 plays a critical role in host responses against mycobacterial infection. Collectively, these findings indicate that Dectin-2 acts as a functional PRR for mycobacterial Man-LAM.

## RESULTS

### LAM Promotes Experimental Autoimmune Encephalomyelitis through FcRγ

We first investigated whether LAM possess adjuvant activity in vivo. To this end, we performed a murine model of T-cell-mediated autoimmune disease, experimental autoimmune encephalomyelitis (EAE) (Figures 1A–1D). Mice were immunized with myelin oligodendrocyte glycoprotein (MOG) peptide together with LAM derived from virulent *M. tuberculosis* strain Aoyama B. Although EAE was not induced by incomplete Freund's adjuvant (IFA) alone (data not shown), a single injection of LAM elicited EAE with 100% incidence (Figures 1A and 1B). The EAE symptoms were completely abrogated in *Fcer1g*$^{-/-}$ mice (Figures 1A and 1B), suggesting that FcRγ-coupled receptor(s) might contribute to LAM-induced EAE. Furthermore, in contrast to lymphocytes from wild-type mice, lymphocytes from *Fcer1g*$^{-/-}$ mice exhibited impaired ex vivo recall responses to MOG peptides as judged by the production of IL-17, interferon-γ (IFN-γ), and granulocyte macrophage-colony stimulating factor (GM-CSF) (Figures 1C and 1D). These results indicate that LAM could act as a potent adjuvant leading to the development of EAE through an FcRγ-dependent pathway.

Because FcRγ is mainly expressed in myeloid cells, we next treated DCs with LAM in vitro. To recapitulate uniform configuration and multivalency of LAM on the bacterial wall, LAM was coated on culture plate for the stimulation of bone-marrow-derived DCs (BMDCs). Although soluble LAM did not induce cytokine production (data not shown), plate-coated LAM could stimulate BMDCs to secrete a large amount of the proinflammatory cytokines, macrophage inflammatory protein-2 (MIP-2), and

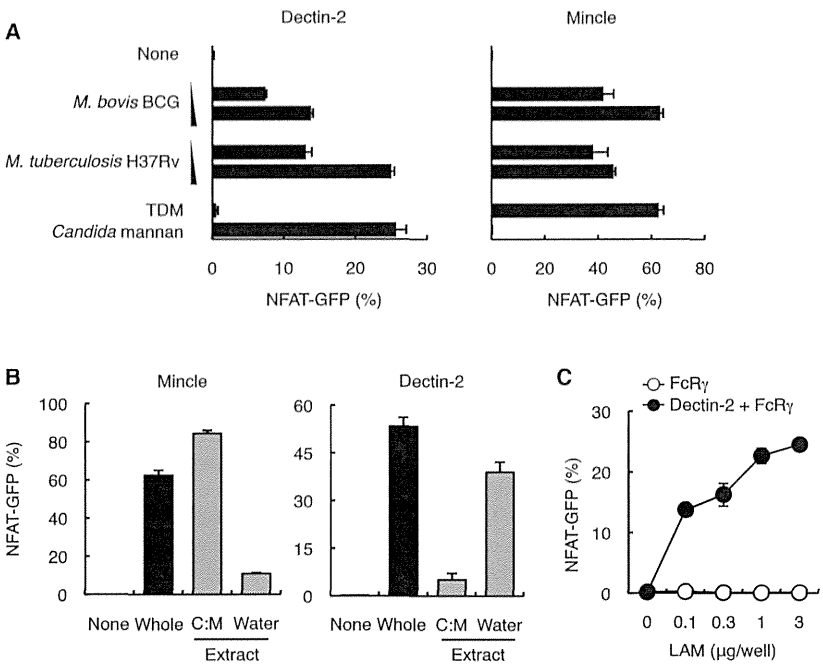


**Figure 2. Dectin-2 Recognizes Pathogenic Mycobacterial Species though LAM**

(A) NFAT-GFP reporter cells expressing Mincle + FcRγ (Mincle) or Dectin-2 + FcRγ (Dectin-2) were stimulated with heat-killed *M. tuberculosis* H37Rv or *M. bovis* BCG. TDM and *Candida albicans* cell wall mannan were used in plate-coated form as a positive control.

(B) Reporter cells were stimulated with plate-coated water extract or C:M extract for 24 hr.

(C) Reporter cells expressing FcRγ alone or Dectin-2 + FcRγ were stimulated with the indicated amounts of LAM derived from *M. tuberculosis* strain Aoyama B in plate-coated form for 24 hr.

Induction of NFAT-GFP was analyzed using flow cytometry. All data are presented as the means ± SD of triplicate assays and representative results from three independent experiments with similar results are shown. See also Figure S2.

TNF (Figures 1E and 1F). These cytokines were still produced in *Clec4e*$^{-/-}$ (Figures 1E and 1F) and *Clec4d*$^{-/-}$ (data not shown) DCs. MyD88 was dispensable for this response, indicating that toll-like receptors (TLRs) do not play major role in LAM recognition. In contrast, LAM-induced cytokine production was abrogated in *Fcer1g*$^{-/-}$ DCs. These results suggest that some unknown FcRγ-coupled receptor(s) might function as an activating receptor for LAM in BMDCs.

### Dectin-2 Recognizes Mycobacterial LAM

Mincle, MCL, and Dectin-2 are FcRγ-coupled activating receptors within the same gene cluster, and two of these receptors, Mincle and MCL, recognize mycobacteria (Ishikawa et al., 2009; Miyake et al., 2013). We therefore assumed that Dectin-2 might also be evolved as a receptor for mycobacteria. Indeed, Dectin-2 was demonstrated to recognize the virulent strain *M. tuberculosis* H37Rv and the vaccine strain *M. bovis* Bacille de Calmette et Guérin (BCG) to activate the reporter cells, in a similar manner to Mincle (Figure 2A). However, the ligand for Dectin-2 was distinct from Mincle ligand trehalose-6,6′-dimycolate (TDM) (Figure 2A).

We next fractionated components of *M. bovis* BCG using lipophilic and hydrophilic solvents, such as chloroform:methanol (C:M) and water. The Dectin-2 ligand activity for each of the extracts was assessed in a plate-coated form using reporter cells. We found that only the water phase demonstrated a stimulatory activity for Dectin-2 (Figure 2B, right), in sharp contrast to the C:M phase that activates Mincle-expressing cells (Figure 2B, left) (Ishikawa et al., 2009). These results suggest that the hydrophilic components of mycobacteria are candidates for the Dectin-2 ligand. Among mycobacterial hydrophilic components, LAM constitutes the most abundant hydrophilic lipoglycan (Figure S1 available online; Leopold and Fischer, 1993). In agreement with our prediction, LAM derived from *M. tuberculosis* activated reporter cells expressing Dectin-2 (Figure 2C). Dectin-2 directly recognized the LAM, as shown by the fact that soluble Dectin-2 protein (Dectin-2-Ig) bound to purified LAM in a dose-dependent manner (Figure S2). These findings indicate that Dectin-2 is a direct receptor for mycobacterial LAM.

### Dectin-2 Recognizes Mycobacteria through Mannose-Capped LAM

The structure of LAM differs depending on the mycobacterial species, particularly with the respect to the capping moieties (Briken et al., 2004). The slow-growing strains including *M. tuberculosis* and *M. bovis* BCG possess Man-LAM, whereas rapid-growing strains of mycobacteria do not. *M. smegmatis* possesses PI-LAM. To clarify which structure of LAM is responsible for the interaction with Dectin-2, we used various strains of mycobacteria including nontuberculosis mycobacteria (NTM).

Dectin-2 recognized slow-growing strains, such as *M. intracellulare* and *M. gordonae*, which possess Man-LAM. In contrast, Dectin-2 did not recognize *M. abscessus* and *M. smegmatis* that lack mannose capping (Figure 3A). Importantly, Mincle was capable of recognizing these strains (Figure 3A). We confirmed that none of these strains activated reporter cells expressing FcRγ alone (data not shown). These results suggest that Dectin-2 preferentially recognizes the mycobacterial species that express Man-LAM. Supporting this notion, the activity of Man-LAM derived from *M. tuberculosis* (Figure 2C) was abolished by treatment with α-mannosidase that removes terminal mannose caps (Figure 3B). These results indicate that the capping structures are crucial determinants for the recognition of Man-LAM by Dectin-2.

We next investigated whether the mannose binding capacity of Dectin-2 is involved in Man-LAM recognition. To this end, we employed the Dectin-2$^{QPD}$ mutant in which the mannose-binding activity was eliminated by substituting EPN (glutamic acid-proline-asparagine) sequence into galactose-type QPD (glutamine-proline-asparagic acid) sequence (Drickamer,

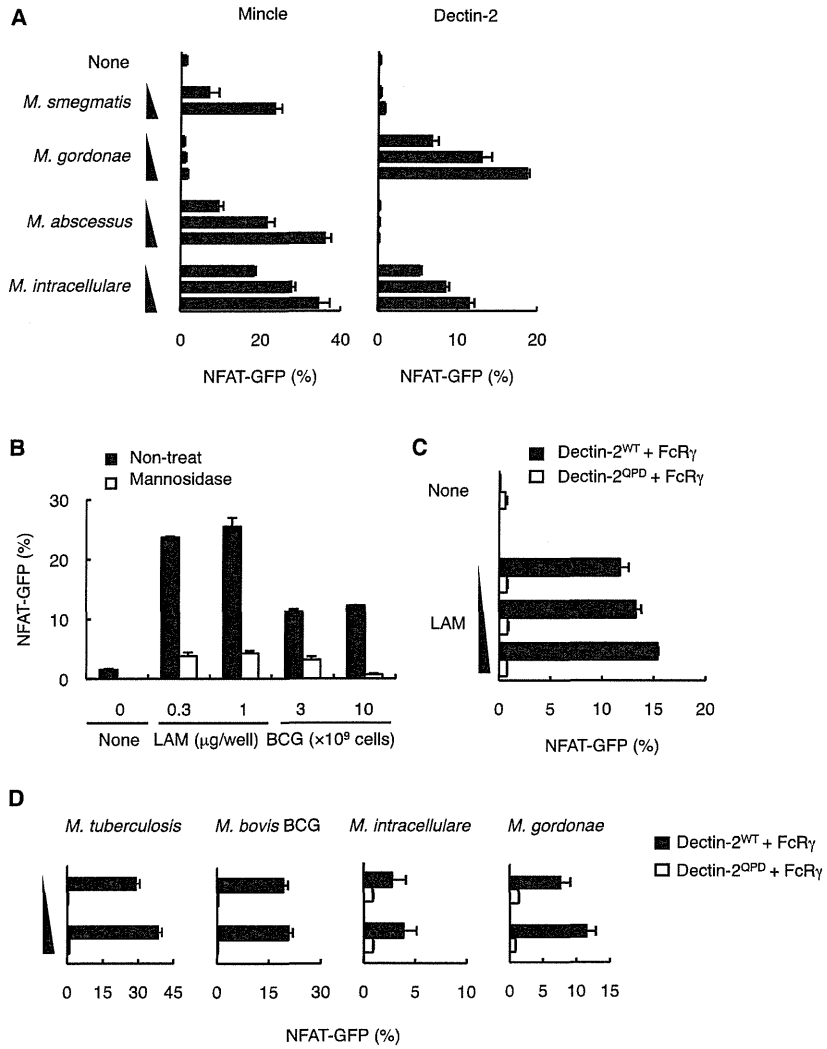


**Figure 3. Dectin-2 Selectively Recognizes Mannose-Capped LAM**

(A) NFAT-GFP reporter cells expressing Mincle + FcRγ or Dectin-2 + FcRγ were stimulated with the indicated strains of heat-killed NTM.

(B) Reporter cells expressing Dectin-2 + FcRγ were stimulated with *M. bovis* BCG pretreated with or without α-mannosidase for 24 hr.

(C and D) Reporter cells expressing Dectin-$2^{WT}$ + FcRγ or Dectin-$2^{QPD}$ + FcRγ were stimulated with plate-coated LAM (C) and NTM strains (D) for 24 hr.

All data are presented as the means ± SD of triplicate and are representative of three separate experiments. See also Figure S3.

1992; Ishikawa et al., 2013). Man-LAM did not activate reporter cells expressing Dectin-$2^{QPD}$ (Figure 3C) regardless of similar fluorescence intensities of wild-type Dectin-2 and Dectin-$2^{QPD}$ on the cell surface (Figure S3). The recognition of whole mycobacteria by Dectin-2 was also dependent on this EPN motif (Figure 3D). Collectively, these results indicate that both mannose caps of Man-LAM and mannose-recognition property of Dectin-2 are required for the interaction of Man-LAM with Dectin-2.

### Man-LAM Induces Cytokine Production by DCs in a Dectin-2-Dependent Manner

Among the myeloid cells, DCs most abundantly express Dectin-2 (Ariizumi et al., 2000). We therefore investigated the cytokine production in response to Man-LAM in BMDCs. Man-LAM, similar to TDM, induced the expression of inflammatory cytokines, such as MIP-2, TNF, and IL-6, in a dose-dependent manner (Figure 4A). The LAM-induced cytokine production was abolished in *Clec4n*$^{-/-}$ BMDCs, whereas the TDM-mediated cytokine production was not altered (Figure 4A). Man-LAM also slightly enhanced IL-12p40 in a Dectin-2-dependent manner (data not shown). The production of TNF and IL-6 upon *M. bovis* BCG infection was partially decreased in *Clec4n*$^{-/-}$ BMDCs as compared with WT BMDCs, although there remained Dectin-2-independent cytokine production (Figure 4B). These data indicate that Dectin-2 is critical for Man-LAM-mediated proinflammatory cytokine production in DCs.

We next focused on the anti-inflammatory potential of Man-LAM-Dectin-2 pathway, due to the fact that accumulating evidence has emphasized the importance of the immune-suppressive action of Man-LAM (Geijtenbeek et al., 2003; Wieland et al., 2007). In addition to proinflammatory cytokines, Man-LAM potently induced the production of anti-inflammatory cytokine, IL-10, in BMDCs (Figure 4C, left). Other pathogen-associated molecular patterns (PAMPs), TDM (Figure 4C, right) and LPS (data not shown), did not induce the secretion of IL-10 and IL-2, indicating that Man-LAM has a unique profile of the cytokine production. Man-LAM-induced release of these cytokines was completely suppressed in *Clec4n*$^{-/-}$ BMDCs (Figure 4C). Although TNF production during *M. bovis* BCG infection was partially dependent on Dectin-2 as described above (Figure 4B), the production of IL-10 and IL-2 was almost completely lost in *Clec4n*$^{-/-}$ DCs infected with *M. bovis* BCG (Figure 4D). Meanwhile, *M. abscessus*, which is absent from mannose caps, failed to induce the production of IL-10 and IL-2, compared to the capability of MIP-2 production (Figure 4E). These results suggest a central role of Dectin-2 in the production of IL-10 and IL-2 in response to mycobacteria.

### Dectin-2-Mediated Intrinsic Signal Regulates Man-LAM-Induced Cytokine Production in DCs

It is clear that Dectin-2 is required for the cytokine production induced by Man-LAM, because such production is abrogated in *Clec4n*$^{-/-}$ cells (Figures 4A and 4C). However, it is still

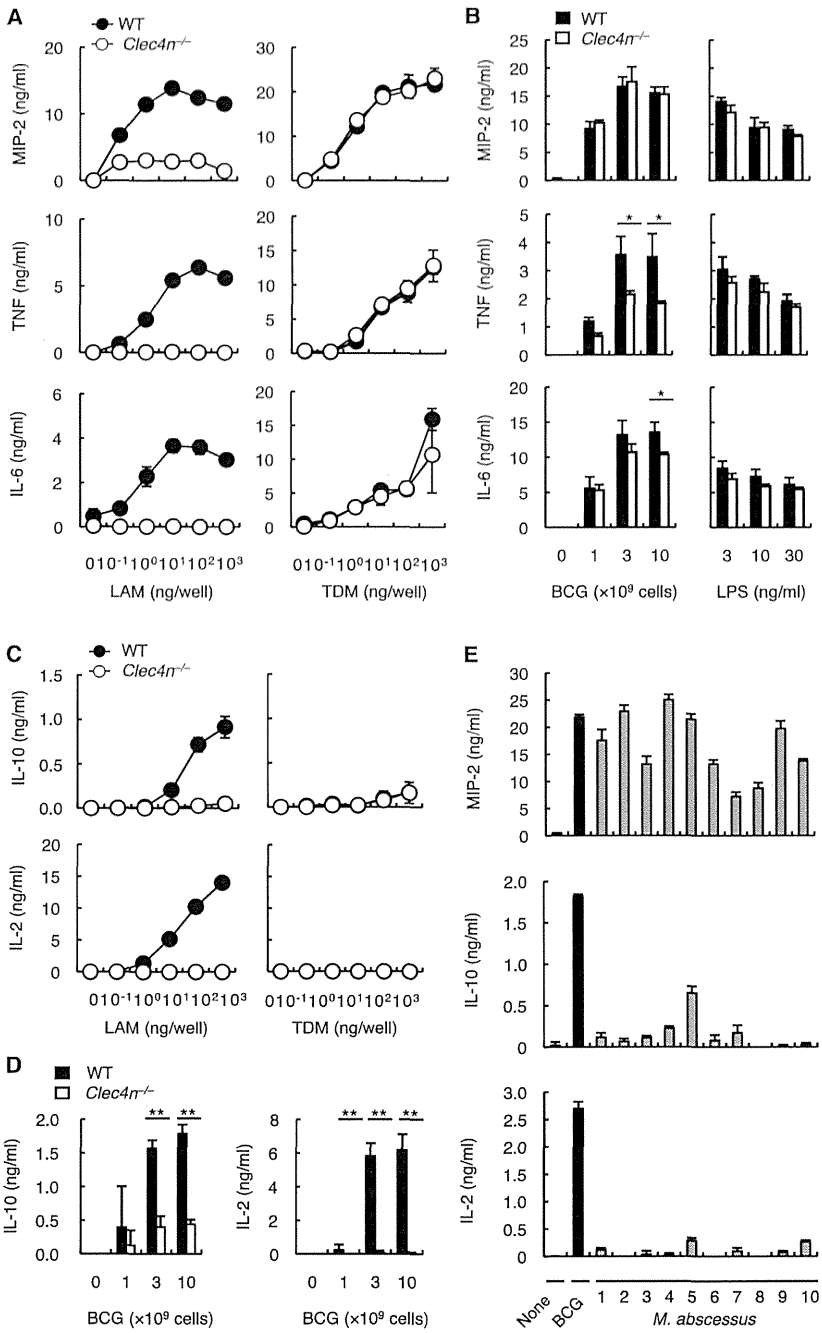


**Figure 4. LAM Induces Cytokine Production in a Dectin-2-Dependent Manner**

(A–D) BMDCs obtained from WT or *Clec4n*$^{-/-}$ mice were stimulated with the indicated amounts of plate-coated LAM or TDM for 48 hr (A and C). BMDCs were infected with 1 to 10 × $10^9$ of *M. bovis* BCG for 48 hr (B and D). LPS was used as control. The concentrations of MIP-2, TNF, IL-6 (A and B), IL-10, and IL-2 (C and D) were measured using ELISA.

(E) BMDCs were stimulated for 48 hr with *M. bovis* BCG or clinical isolates of heat-killed *M. abscessus* derived from ten individual patients. The concentrations of MIP-2, IL-10, and IL-2 were measured using ELISA.

All data are presented as the means ± SD of triplicate and are representative of three separate experiments. See also Figure S4.

uncertain whether the Dectin-2-mediated intrinsic signal is sufficient or whether some other coreceptor is also required for these responses. The unique cytokine profiles, particularly IL-10 and IL-2 production, may be conferred by the coengagement of Dectin-2 and other Man-LAM receptors. To examine this possibility, we investigated the contribution of several candidate receptors for Man-LAM. Since SIGNR1, a putative murine homolog of human DC-SIGN, recognizes Man-LAM (Koppel et al., 2004), we evaluated the role of SIGNR1 by establishing SIGNR1-deficient mice (Figure S4A). However, BMDCs lacking SIGNR1 were still capable of producing all cytokines tested at amounts comparable to those in WT BMDCs (Figure S4B). Another DC-SIGN homolog, SIGNR3, which is expressed in a limited population of myeloid cells (Nagaoka et al., 2010), was not detected in BMDCs (Figure S4C). Furthermore, forced expression of SIGNR3 in BMDCs did not increase Man-LAM-induced cytokine production (Figure S4D). Notably, *Clec4n*$^{-/-}$ BMDCs failed to produce cytokines even with the expression of SIGNR3 (Figure S4D). These results collectively indicate that both SIGNR1 and SIGNR3 are not essential for cytokine production induced by Man-LAM in BMDCs.

Macrophage mannose receptor (MMR) could also bind to Man-LAM (Nigou et al., 2001). Because MMR expression was detected in BMDCs (Figure S4C), we assessed its role in Man-LAM-induced cytokine release by using anti-MMR blocking monoclonal antibody (mAb). However, the mAb treatment did not influence the production of IL-10 and IL-2 in BMDCs (Figure S4E).

A recent report has shown that Dectin-2 is capable of associating with MCL (Zhu et al., 2013). Meanwhile, analyses of *Clec4d*$^{-/-}$ BMDCs revealed that MCL is not required for the Man-LAM-induced cytokine production (Figure S4F). Man-LAM is weakly recognized by TLR2 and TLR4 (Mazurek et al., 2012). However, IL-10 production induced by Man-LAM was not altered in *MyD88*$^{-/-}$ BMDCs (Figure S4G), suggesting that TLR-MyD88 signaling does not play a major role in the effect of Man-LAM. Finally, we confirmed that the direct engagement of Dectin-2 alone by anti-Dectin-2 cross-linking replicated the production of IL-10 (Figure S4H).

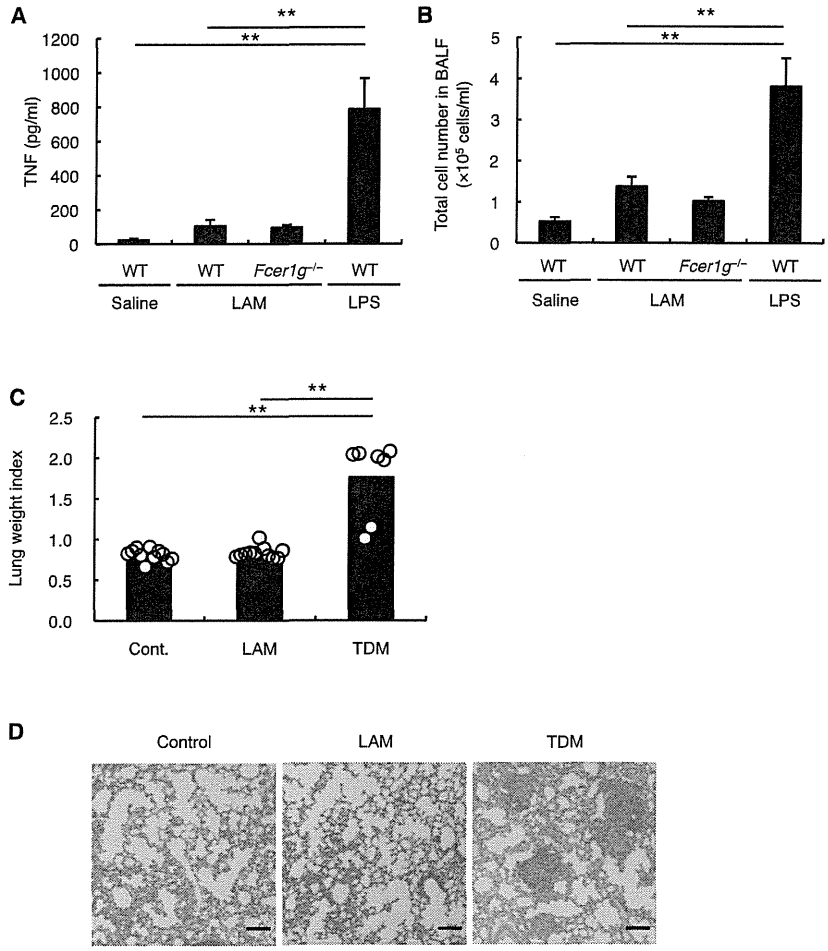


**Figure 5. LAM Does Not Cause Excessive Inflammation in the Lungs**

(A and B) Mice were intratracheally administered 100 μg of LAM (WT, n = 13; *Fcer1g*$^{-/-}$, n = 5), 10 μg of LPS (WT, n = 9), or 100 μl of sterile saline as a control (WT, n = 7). After 8 hr, BALF was obtained and then TNF concentrations in the BALF were determined using ELISA (A). The number of total cells was determined by hemocytometer (B). All data are presented as the means ± SD.

(C) Lungs of control mice (Cont., n = 11), 50 μg of LAM (LAM, n = 11)- or 50 μg of TDM (TDM, n = 7)-injected mice were isolated at day 7 and inflammatory intensity was evaluated by calculation of lung weight index. Each symbol represents an individual mouse. Data are representative of three separate experiments.

(D) Histology of the lungs from control, LAM (50 μg)-, or TDM (50 μg)-injected mice were was examined by hematoxylin-eosin staining at day 7. Scale bars represent 0.1 mm. Data are representative of three separate experiments.

Collectively, these results suggest that the IL-10-inducing potential of Man-LAM is likely due to the intrinsic properties of Dectin-2-mediated signaling.

### Man-LAM Induces Minimal Inflammation In Vivo

To investigate whether Man-LAM triggers any inflammatory responses, we evaluated the response of mice to Man-LAM administration in vivo. The infiltration of inflammatory cells and cytokine production in bronchoalveolar lavage fluid (BALF) was examined following the intratracheal administration of LAM or LPS (Figures 5A and 5B). LPS induced a significant increase in TNF production and cell infiltration in WT mice. In contrast, Man-LAM did not induce marked inflammatory responses. Consistent with this observation, FcRγ deficiency had no apparent effect compared with Man-LAM-treated WT mice.

Intravenous injection of TDM induced inflammatory lung swelling as assessed by lung weight index (LWI) (Figure 5C) and granuloma formation in lungs (Figure 5D, right) as previously reported (Ishikawa et al., 2009). In contrast, the same amount of Man-LAM induced neither lung swelling (Figure 5C) nor granuloma formation (Figure 5D, middle). These results indicate that Man-LAM does not induce strong pulmonary inflammation compared with other PAMPs such as TDM or LPS.

### Man-LAM Stimulation Enhances APC Functions to Promote IL-17 Production In Vitro

We further evaluated the adjuvant activity of Man-LAM in vitro. To investigate the effect of Man-LAM on DC maturation, we examined the expression of costimulatory molecules on BMDCs after Man-LAM stimulation. Man-LAM stimulation upregulated the expression of CD40 and CD80 on WT BMDCs, which were comparable to those induced by LPS (Figure 6A). However, the induction of these costimulatory molecules was abolished in the absence of Dectin-2 and its subunit FcRγ (Figure 6A). Mincle was dispensable for the LAM-induced responses. We confirmed that the LPS-mediated responses were not altered in these mice. These results demonstrate that Man-LAM promotes DC maturation in a Dectin-2-dependent manner.

We next examined the function of antigen-presenting cells (APCs) upon Man-LAM stimulation. BMDCs were pulsed with the ovalbumin (OVA) antigen peptides and cocultured with T cells obtained from OVA-specific OT-II TCR transgenic mice in the presence or absence of Man-LAM. Because T cells do not express Dectin-2 (Ariizumi et al., 2000), this system enables us to evaluate the role of Man-LAM in APC functions toward T cell priming and activation. The antigen-specific secretion of IL-17 from CD4$^{+}$ OT-II T cells was significantly augmented when the cells were cocultured with Man-LAM-treated APCs (Figure 6B). However, this enhancement was markedly attenuated when *Clec4n*$^{-/-}$ APCs were used. The antigen-induced T cell proliferation, as assessed by CFSE dilution, was observed regardless of Dectin-2 expression on DCs (Figure 6B, bottom). The concentration of IL-10 in coculture supernatant was increased depending on the antigen dose, suggesting the generation of IL-10-producing T cells in the presence of DCs stimulated through Man-LAM-Dectin-2 axis (Figure 6B).